

Formulating a Particle-Free and Low Temperature Nickel
Reactive Ink for Inkjet Printing Conductive Features

by

Dylan DeBruin

A Thesis Presented in Partial Fulfillment
of the Requirements for the Degree
Master of Science

Approved April 2019 by the
Graduate Supervisory Committee:

Konrad Rykaczewski, Co-Chair
Cesar Torres, Co-Chair
Owen Hildreth

ARIZONA STATE UNIVERSITY

May 2019

ABSTRACT

Reactive inkjet printing (RIJP) is a direct-write deposition technique that synthesizes and patterns functional materials simultaneously. It is a route to cheap fabrication of highly conductive features on a versatile range of substrates. Silver reactive inks have become a staple of conductive inkjet printing for application in printed and flexible electronics, photovoltaic metallization, and more. However, the high cost of silver makes these less effective for disposable and low-cost applications.

This work aimed to develop a particle-free formulation for a nickel reactive ink capable of metallizing highly pure nickel at temperatures under 100 °C to facilitate printing on substrates like paper or plastic. Nickel offers a significantly cheaper alternative to silver at slightly reduced bulk conductivity.

To meet these aims, three archetypes of inks were formulated. First were a set of glycerol-based inks temperature ink containing nickel acetate, hydrazine, and ammonia in a mixture of water and glycerol. This ink reduced between 115 – 200 °C to produce slightly oxidized deposits of nickel with carbon content around 10 wt %.

The high temperature was addressed in a second series, which replaced glycerol with lower boiling glycols and added sodium hydroxide as a strong base to enhance thermodynamics and kinetics of reduction. These inks reduced between 60 and 100 °C but sodium salts contaminated the final deposits.

In a third set of inks, sodium hydroxide was replaced with tetramethylammonium hydroxide (TMAH), a strong organic base, to address contamination. These inks also reduced between 60 and 100 °C. Pipetting or printing onto gold coated substrates produce metallic flakes coated in a clear, thick residue. EDS measured carbon and oxygen content

up to 70 wt % of deposits. The residue was hypothesized to be a non-volatile byproduct of TMAH and acetate.

Recommendations are provided to address the residue. Ultimately the formulated reactive inks did not meet design targets. However, this thesis sets the framework to design an optimal nickel reactive ink in future work.

ACKNOWLEDGMENTS

I would foremost like to thank my advisor, Professor Owen Hildreth. I am greatly appreciative for the opportunity to work with him in such a fascinating and encouraging field. This project has been invaluable to the development of my career interests and has challenged me to learn a diverse array of knowledge and skills. I am confident that what I've learned here will enable future success as I pursue a career in engineering.

I would like to thank my committee members, Professors Konrad Rykaczewski and Cesar Torres for their advice and support throughout this work. I am deeply grateful for Dr. Rykaczewski allowing me to finish my research in his lab the last two semesters, and for being so accommodating along the way.

I would also like to acknowledge Professor Ryan Trovitch for taking the time to help me understand some of the intricate chemistry seen in this work. His help led me to findings that I don't think I could have reached on my own.

I am deeply appreciative of the members of both Professors Hildreth and Rykaczewski's research groups. I would like to thank Avinash and Subbarao for all their support throughout this project, and especially during my visit to Colorado. I am especially appreciative of Subbarao for assisting with printing and analyzing samples after I left. I could not have finished without this. I would like to thank Chad for being so accommodating when I moved into the new lab, and for all the discussions that aided me in solving some of the obstacles that I ran into during this work.

TABLE OF CONTENTS

	Page
LIST OF TABLES.....	v
LIST OF FIGURES	vi
CHAPTER	
1 INTRODUCTION	1
Problem Statement and Scope.....	3
Thesis Organization	3
2 LITERATURE REVIEW	4
Organization	4
Conductive Inks	4
Reactive Inkjet Printing Using Organometallic Inks	7
Electroless Nickel	10
Summary	13
3 METHODOLOGY	15
Chemicals	15
Ink Deposition Test Methods.....	15
Sealed Vial Test Methods.....	16
Product Characterization Methods	18
4 TESTING HYDRAZINE AS A REDUCTANT FOR INKS	19
Introduction	19
Proof of Concept.....	20
Preliminary Pipette Tests with Hydrazine.....	21

CHAPTER	Page
Testing Approaches to Facilitating Reduction	22
Summary	25
5 HIGH TEMPERATURE GLYCEROL-SOLVATED INKS	26
Introduction	26
Screening Polyols.....	26
Glycerol-Solvated Inks.....	28
Glycerol-Solvated Inks with Addition of an Inductant	30
Summary	33
6 TRANSITIONING TO LOW TEMPERATURE INKS	34
Introduction	34
Screening Low Temperature Solvents.....	34
Chemistry Studies	39
Low Temperature Inks in Strongly Basic Media.....	46
Byproducts Study.....	55
Summary	58
7 LOW TEMPERATURE INKS USING TMAH AND PROPYLENE GLYCOL	59
Introduction	59
Proof of Concept: Sealed Vial Tests Employing TMAH.....	60
Pipetting Enhanced PG Inks Using TMAH as a Base	62
Printing Enhanced PG Inks Using TMAH as a Base.....	64
Analyzing Deposition on Glass.....	70

CHAPTER	Page
Summary	74
8 CONCLUSIONS AND FUTURE WORK	75
Summary of Results	75
Recommendations.....	78
REFERENCES	83

LIST OF TABLES

Table	Page
1. EDS Elemental Weight and Atomic Distributions in Deposit Produced by Pipetting a Glycerol-Based Ink onto a Gold-Coated Glass Slide.....	29
2. EDS-Sourced Elemental Composition of Deposit Produced with a Glycerol-Based Ink Containing Inductant	32
3. Atomic and Weight Distributions of the White Material	41
4. Complexes Formed by Mixing 0.1 M Nickel Acetate Tetrahydrate in Common Solvents at Ambient Conditions.....	42
5. EDS Analysis of pH-Enhanced NH ₃ Ink Deposits	50
6. EDS-Sourced Distribution of Elements in Deposit Produced by First pH-Enhanced PG Ink.....	53
7. EDS-Sourced Distribution of Elements in Deposit Produced by Second pH-Enhanced PG Ink.....	54
8. EDS-Sourced Distribution of Elements in Deposit Produced by Third pH-Enhanced PG Ink.....	55
9. EDS-Sourced Elemental Distribution in Byproduct Produced by Evaporating Propylene Glycol with Dissolved Sodium Hydroxide	58
10. Elemental Weight and Atomic Distributions in Deposit Produced by Printing Ink Containing DI Water and TMAH onto Gold-Coated Silicon.....	66
11. Elemental Weight and Atomic Distributions in Deposit Produced by Printing Ink Containing Ammonia and TMAH onto Gold-Coated Silicon.....	68

Table	Page
12. Elemental Weight and Atomic Distributions in Deposit Produced by Printing Ink Containing Ethylamine and TMAH onto Gold-Coated Silicon.....	70
13. Elemental Weight and Atomic Distributions in Deposit Produced by Printing Ink Containing Ethylamine and TMAH onto Gold-Coated Glass.....	72

LIST OF FIGURES

Figure	Page
1. XRD Pattern of Nickel Sample Synthesized Using Hydrazine as a Reductant at 60 °C in a 20/80 Vol % Mixture of Water and Ammonia Solution	21
2. Optical Image of Hydrazine-Based Ink Pipetted onto a Glass Slide At 60 °C.....	21
3. Common Products of Nickel Reactive Inks Containing Nickel Acetate, Hydrazine, Ammonia, Water, and Simple Alcohol or Amine-Based Solvents.....	23
4. Top and Bottom Views of Deposit Produced by Pipetting Water-Based Ink onto a Glass Slide	25
5. Dried Droplets of Ink Pipetted onto Untreated Glass	27
6. Dried Droplets of Ink Pipetted onto Gold-Coated Glass.....	27
7. Optical Images of Deposit Produced by Pipetting a Glycerol-Based Ink onto a Gold-Coated Glass Slide	29
8. SEM of Deposit Produced by Pipetting a Glycerol-based Ink onto a Gold-Coated Glass Slide	29
9. Deposit Produced by Pipetting Glycerol-Solvated Ink Containing 0.1 M Ni(CH ₃ CO ₂) ₂ , 3.6 M 2H ₄ , and 0.015 M NaH ₂ PO ₂ onto Gold-Coated Glass At 125 °C	30
10. SEM of Deposit Produced by Pipetting Glycerol-Solvated Ink Containing 0.1 M Ni(CH ₃ CO ₂) ₂ , 3.6 M 2H ₄ , and 0.015 M NaH ₂ PO ₂ onto Gold-Coated Glass.....	31
11. SEM of Crystals Embedded on Deposit Produced by Pipetting Glycerol-Solvated Ink Containing 0.1 M Ni(CH ₃ CO ₂) ₂ , 3.6 M 2H ₄ , and 0.015 M NaH ₂ PO ₂ onto Gold-Coated Glass.....	31

Figure	Page
12. FTIR of Deposit Produced by Pipetting Glycerol-Solvated Ink Containing 0.1 M Ni(CH ₃ CO ₂) ₂ , 3.6 M 2H ₄ , and 0.015 M NaH ₂ PO ₂ onto Gold-Coated Glass.....	32
13. Optical Images of Deposits Produced by Pipetting an NH ₃ -Based Ink (0.05 M [Ni ²⁺], 1.8 M [N ₂ H ₄], And 12.3 M [NH ₃] in Water) onto Gold-Coated Glass	36
14. Optical Images of Deposits Produced by Pipetting an NH ₃ -Based Ink (0.10 M [Ni ²⁺], 1.8 M [N ₂ H ₄], And 12.3 M [NH ₃] in Water) onto Gold-Coated Glass	36
15. Optical Images of PG-Based Ink (0.05 M [Ni ²⁺] and 1.5 M [N ₂ H ₄] in 33.3 Vol % DI Water and 66.7 Vol % PG). Droplets Were Pipetted onto Gold-Coated Glass	37
16. Optical Images of EG-Based Ink (0.05 M [Ni ²⁺] and 1.5 M [N ₂ H ₄] in 16.7 Vol % DI Water and 83.3 Vol % PG). Droplets Were Pipetted onto Gold-Coated Glass	38
17. Optical Imagery of the Bulk White Material.....	39
18. SEM of the Bulk Regions of the White Material	40
19. SEM of the Boundary Region of the White Material	40
20. 0.5 M Nickel Acetate Tetrahydrate in 35 wt % Hydrazine Solution in Water, Before and After Lightly Shaking, Showing What Is Hypothesized to Be a Polymerization Reaction of a Nickel-Hydrazine Complex	42
21. Sealed Vessels Containing 0.1 M [Ni ²⁺], 3.0 M [N ₂ H ₄], and 0.4 M [NaOH] in 50 vol % of Primary Solvent and 50 vol % of H ₂ O.....	48
22. Optical Images of pH-Enhanced NH ₃ Ink Pipetted onto Gold-Coated Silicon at 60 °C Containing 1.8 M [N ₂ H ₄] and 0.4 M [NaOH]	49
23. Optical Images of PG-Based Inks Pipetted onto Gold-Coated Silicon at 75 °C	51
24. . SEM of First pH-Enhanced PG-Based Ink	52

Figure	Page
25. SEM of Second pH-Enhanced PG-Based Ink	53
26. SEM of Third pH-Enhanced PG-Based Ink.....	54
27. Residues Produced by Drying Sodium Hydroxide in Various Solvents	56
28. SEM of Residue Produced by Drying Sodium Hydroxide in Propylene Glycol	57
29. XRD Scans of Samples Synthesized in Sealed Vials at 60 °C Using the Formulation 0.05 M [Ni ²⁺], 2.2 M [N ₂ H ₄], and 0.28 M [TMAH] in 30/30/40 vol % mix of DI water, Primary Solvent, and Propylene Glycol.....	61
30. Overlaid XRD of Samples Synthesized in Sealed Vial Tests at 60 °C	61
31. Deposits Produced by Pipetting Inks (0.05 M [Ni ²⁺], 1.84 M [N ₂ H] And 0.4 M [TMAH] in a 20/30/50 vol % Mix of DI Water, Primary Solvent, and PG, Respectively) onto a Gold-Coated Glass Slide at 75 °C	63
32. Deposits Produced by Pipetting Inks (0.05 M [Ni ²⁺], 1.84 M [N ₂ H] And 0.4 M [TMAH] in a 20/30/50 vol % Mix of DI Water, Primary Solvent, and PG, Respectively) onto a Gold-Coated Glass Slide at 100 °C	63
33. Images of Deposits Produced by Printing Ink (0.05 M [Ni ²⁺], 1.84 M [N ₂ H ₄] and 0.4 M [TMAH] in a 50/50 vol % Mix of DI Water and PG) at 75 °C onto Gold-Coated Substrates	65
34. Images of Deposits Produced by Printing Ink (0.05 M [Ni ²⁺], 1.84 M [N ₂ H ₄] and 0.4 M [TMAH] in a 50/50 vol % Mix of DI Water and PG) at 100 °C onto Gold-Coated Substrates	65

Figure	Page
35. SEM of Deposits Produced by Printing Ink (0.05 M [Ni ²⁺], 1.84 M [N ₂ H ₄] and 0.4 M [TMAH] in a 50/50 vol % Mix of DI Water and PG) at 100 °C onto Gold-Coated Silicon	65
36. Images of Deposits Produced by Printing Ink (0.05 M [Ni ²⁺], 1.84 M [N ₂ H ₄] and 0.4 M [TMAH] in a 20/30/50 vol % Mix of DI Water, Ammonia Solution, and PG) at 75 °C onto Gold-Coated Substrates	67
37. Images of Deposits Produced by Printing Ink (0.05 M [Ni ²⁺], 1.84 M [N ₂ H ₄] and 0.4 M [TMAH] in a 20/30/50 vol % Mix of DI Water, Ammonia Solution, and PG) at 100 °C onto Gold-Coated Substrates	67
38. SEM of Deposits Produced by Printing Ink (0.05 M [Ni ²⁺], 1.84 M [N ₂ H ₄] and 0.4 M [TMAH] in a 20/30/50 vol % Mix of DI Water, Ammonia Solution, and PG) at 100 °C onto Gold-Coated Silicon	67
39. Images of Deposits Produced by Printing Ink (0.05 M [Ni ²⁺], 1.84 M [N ₂ H ₄] and 0.4 M [TMAH] in a 20/30/50 vol % Mix of DI Water, Ethylamine Solution, and PG) at 75 °C onto Gold-Coated Substrates	69
40. Images of Deposits Produced by Printing Ink (0.05 M [Ni ²⁺], 1.84 M [N ₂ H ₄] and 0.4 M [TMAH] in a 20/30/50 vol % Mix of DI Water, Ethylamine Solution, and PG) at 100 °C onto Gold-Coated Substrates	69
41. SEM of Deposits Produced by Printing Ink (0.05 M [Ni ²⁺], 1.84 M [N ₂ H ₄] and 0.4 M [TMAH] in a 20/30/50 vol % Mix of DI Water, Ethylamine Solution, and PG) at 100 °C onto Gold-Coated Silicon	69

Figure	Page
42. SEM of Deposits Produced by Printing Ink (0.05 M [Ni ²⁺], 1.84 M [N ₂ H ₄] and 0.4 M [TMAH] in a 20/30/50 vol % Mix of DI Water, Ethylamine Solution, and PG) at 100 °C onto Gold-Coated Glass	71
43. Elemental Spot Maps Composed by EDS on Deposit Produced by Printing Ink (0.05 M [Ni ²⁺], 1.84 M [N ₂ H ₄] and 0.4 M [TMAH] in a 20/30/50 vol % Mix of DI Water, Ethylamine Solution, and PG) at 100 °C onto Gold-Coated Glass.....	71

CHAPTER 1

INTRODUCTION

Reactive inkjet printing is a direct write deposition technique for functional materials which synthesizes a material simultaneous to patterning its structure. The technique is of interest for its material efficiency and low processing cost relative to other patterning techniques, as well as its ability to fabricate a versatile array of materials.^{1,2} This work focuses specifically on printing conductive features for use in direct metallization applications like photovoltaics, microfluidic devices, printable electronics, biosensors³, and even tissue engineering.^{4,5}

Early work in conductive inkjet printing has printed polymeric, colloidal, and organometallic inks to fabricate conductive features.^{6,7,8} Conductive polymers tend to be less conductive than metals, and the corresponding inks exhibit Non-Newtonian behaviors when concentrated, complicating the printing process. Colloidal inks similarly hinder printability via issues like nozzle clogging caused by agglomeration. Colloidal inks also require high temperature sintering to bond nanoparticles together in order to increase conductivity. Early organometallic inks metallized via thermal or optical decomposition of a metal-organic complex. These can achieve high conductivities at lower temperatures than nanoparticle inks but the annealing temperature required to drive decomposition is usually too high for thermally-sensitive substrates like paper or plastic, which are of interest in emerging technologies such as flexible electronics.⁷ Thus, there remains a need for particle-free inks which deposit products with electrical conductivities comparable to bulk metals at temperatures at or below 100 °C.

More recent work has transitioned towards direct metallization techniques like the aforementioned organometallic inks to address these issues. Reactive metal inks are particle-free solutions containing organometallic precursors and reagents. Upon printing of the ink, a reaction is thermally, optically, or catalytically activated to metallize the precursor while solvents, byproducts, and remaining agents evaporate. Most commonly, the mechanism of reaction is either decomposition or electrochemical reduction. In both cases, deposition temperature is dictated by the reaction rather than processing steps (e.g. sintering). Thus, reactive inks offer a route to highly conductive metal deposition that is low temperature, particle-free, and highly conductive.⁶

Walker⁹ was one of the first to report a self-reducing reactive ink capable of printing metallic silver with near-bulk conductivity at 100 °C. Since then, silver reactive inks have been thoroughly developed in literature and even brought to industry. The prevalence of silver inks is due to a combination of its excellent electrical properties and its electrochemical stability; at a standard electrode potential of 0.80 V, there is an array of volatile reductants available for silver. The primary disadvantage of silver is high raw material cost. Interest has grown in low cost alternatives like nickel, which is less conductive but significantly cheaper. Nickel also introduces unique properties of its own, and so development of a nickel reactive ink would expand the use of reactive inkjet printing technologies. Thus far, formulation of a particle-free and low temperature ink has been hindered by the poor chemical stability of nickel, which diminishes the range of available reductants. However, application of electroless nickel techniques in other fields have highlighted hydrazine as a potent reductant for producing pure, metallic nickel.

1.1 Problem Statement and Scope

At this time, there are no reported nickel inks that can both reduce at temperatures below 100 °C and produce a pure product. This work aims design particle-free nickel reactive ink using hydrazine as a reductant to produce pure nickel deposits and reduce at temperatures below 100 °C.

Choice of hydrazine exploits nickel-hydrazine chemistries that have been reported extensively in literature on nickel nanoparticle synthesis. Hydrazine is a powerful reductant, having a standard electrode potential of -1.15 V under basic conditions. Moreover, it forms a stable solution with water and boils at 114 °C, making it sufficiently volatile for a low temperature ink.

Ink design was approached by transferring successful approaches to hydrazine-based electrochemical nickel reduction from literature to a reactive ink formulation. Then, a series of modifications were made in order to optimize the ink satisfy the aims regarding product purity and processing temperature.

1.2 Thesis Organization

The thesis begins with a literature review of key related topics. After the review, early work is reported, covering attempts to translate nickel nanoparticle synthesis chemistries directly into reactive ink formulations. Then, some inks which use high temperature to force reduction are studied and characterized to establish a working baseline ink. Next, the nickel-hydrazine system is studied thoroughly in bath and droplet settings to facilitate design of lower temperature inks. Some resultant low temperature inks are reported and characterized. Finally, suggestions are made for future work.

CHAPTER 2

LITERATURE REVIEW

2.1 Organization

To date, there is sparse literature on reactive nickel inks; however, much can be learned from other conductive inks. This chapter aims to identify some standardized approaches to formulating conductive inks, establish the current state of nickel reactive inks, and present alternative routes to synthesis.

In accordance, key literature on conductive inks for inkjet printing is reviewed. This leads to a discussion of reactive inks, with a focus on established silver inks. Then, four reported nickel reactive inks are reviewed to characterize the approaches, strengths, and weaknesses of each. Finally, other fields that utilize electroless nickel techniques are reviewed including electroless nickel plating and nickel nanoparticle synthesis.

2.2 Conductive Inks

Conductive inks are solutions that, when printed onto a suitable substrate, deposit electrically-conductive features. These inks present an economic method for mass fabrication of electronics. Features are constructed additively in contrast to techniques like lithography or etching. This results in efficient material usage.

The various types of conductive inks differ in both composition of ink and mechanism of deposition, but three groups of inks can be established according to the conductive precursor: colloidal inks, polymeric inks, and organometallic inks.⁷

2.2.1 Polymeric Inks

Polymeric inks are a solution of polymer and carrier fluid. Examples of conductive polymers include polyaniline, polypyrrole, polythiophene, or polyphenylene.¹⁰ Among these, a conjugated π -system conducts electrons. Polymeric inks offer extensive tunability and can produce lightweight and malleable material, facilitating emerging fields of flexible and printable electronics. Their conductivities are consistently lower than metals but sufficient for applications such as electronic displays¹¹, sensors¹⁰, and other microelectronics¹². These inks can exhibit non-Newtonian behavior at high concentration and molecular weight which can introduce difficulty in designing print parameters.⁷

2.2.2 Colloidal Inks

Colloidal inks are a multi-phase suspension of nanoparticles in a volatile carrier fluid. The inks are printed uniformly onto a substrate and then sintered together to form a bulk deposit. Reported conductivities are high, but still fall short of bulk.

Colloidal inks most commonly print gold^{13,14} or silver^{15,16}, however they have been used to print copper¹⁷ and nickel as well. The latter two usually require special treatment to prevent oxidation.⁷ Water has often been the carrier fluid, but more recently organic solvents and oils have been incorporated to reduce agglomeration.¹⁵ Sometimes, additives are added for this purpose as well. Agglomeration is the biggest limitation of these inks, as it leads to nozzle clogging and limited shelf-life.

2.2.3 Organometallic Inks

Like colloidal inks, organometallic inks deposit metals. However, organometallic inks are fully solvated inks containing a metal-organic complex as the precursor. This circumvents concerns of agglomeration entirely, easing the printing process. There are several common routes employed to transform the complex into the metal including decomposition and self-reduction. Decomposition inks utilize a complex that, under exposure to heat or radiation, will decompose into the metal and a volatile organic byproduct.¹⁸ Self-reducing inks combine the precursor complex with a volatile reductant to reduce the metal cation out of solution. In both cases, the reaction is initiated by some external effect, whether optical radiation, heat, or catalyst, providing control over the deposition. Customarily, organometallic inks require a post-annealing to enhance the electrical conductivity, which can reach near-bulk values.⁷

Organometallic inks are an ideal ink candidate for printing highly conductive features on thermally-sensitive substrates like paper or plastic. These inks produce metals, making them inherently more conductive than most polymeric inks. Moreover, processing conditions are dictated primarily by the reaction chemistry, providing vast flexibility in design routes to low temperature inks. For instance, a self-reducing ink could be designed to metallize at ambient conditions using a strong and reactive reductant, whereas nanoparticle inks are limited by the need for sintering.¹⁸

The bulk of work in on organometallic inks thus far has focused on metallizing silver, although copper and aluminum have been explored more recently. Silver is ideal because it is the most conductive of metals and is chemically stable. Metals like copper or aluminum are less conductive and are susceptible to oxidation after printing.

2.3 Reactive Inkjet Printing Using Organometallic Inks

As previously described, organometallic inks rely on chemical reactions to transform metal atoms from complex to metallic states. These inks are a subset of reactive inkjet printing (RIJP), a technique that prints solution-based inks that react after printing upon activation by some external source such as heat, light, or catalyst.

RIJP is a material-efficient and direct-write deposition method, alternative to techniques like photolithography, vacuum deposition, and electroless plating to name a common few.^{6,18} Reactive inks are often processed at lower temperatures than comparable nanoparticle inks, enabling printing on papers and plastics. Consequently, they are of great interest to emerging technologies in the flexible electronics fields.

While RIJP can synthesize a vast range of functional materials, this work focuses on metallic inks. Particle-free silver reactive have become a staple in research and industry applications of conductive feature fabrication. In accordance, some unique silver inks are reviewed to study the various approaches taken to chemistry design.

2.3.1 Silver Reactive Inks

Walker¹⁹ was one of the first to report a low temperature reactive silver ink capable of near-bulk conductivities. The formulations combined silver acetate, ammonium hydroxide, and formic acid. Regarding chemistry, ammonia protects nickel ions and deprotonates formic acid to form ammonium formate. When printed onto a heated substrate, the ammonia evaporates, leaving the nickel ions open to reduction by the formate. The result is rapid metallization of silver. After annealing at 100 °C, electrical conductivities up to 90% of bulk were measured. The incorporation ammonia caused low

viscosity and high surface tension, which impeded printability. Walker demonstrated that addition of alkyl amines and primary amines offered a route to mechanical property tuning in order to facilitate printing.

In contrast to Walker, Raut et al.²⁰ chosen reducing ligands to complex with nickel, rather than separate complexing and reducing agents. Similarly, Chen et al.²¹ used silver citrate as a precursor to provide the silver ion and reducing ion together. Both of these works show material-efficient routes to chemistry design which minimize the number of ink components.

Kate et al.²² demonstrated a series of inks utilizing alcohols as catalytic reducing agents to dissociate silver organometallic precursors, preparing them for reduction. In one example, [(hfac)(1,5-COD)Ag] was dissolved in toluene along with propan-2-ol to catalyze a four step reduction of silver upon printing at 120 °C. The resultant silver deposits were highly metallic and featured an electrical resistivity of 39.2 % of bulk.

Yang et al.²³ demonstrated a particularly unique approach to silver inks in which both decomposition and self-reduction mechanisms were utilized to achieve metallization. The two mechanisms were combined in an attempt to organic byproducts commonly produced in the boundary region of organometallic silver reactive inks. However, the inks required a 155 °C sintering step to bind the silver and achieve high conductivities.

2.3.2 Nickel Reactive Inks

There are many reported colloidal inks for printing nickel, but only a few particle-free reactive inks, thus far. Most use an electrochemical reduction mechanism to transform the nickel from complex to metal.

Pasquarelli²⁴ first reported a nickel reactive ink in 2007 that decomposed on glass and ZnO substrates at 140-180 °C to produce metallic nickel, confirmed by XRD. The ink combined a nickel salt precursor, organic solvent, and several organic additives. Once heated, the precursor decomposed to form the metal and an organic by product. Analysis showed a lack of carbon or oxide contamination, indicating that the byproduct evaporated, resulting in high purity. The resistivity was measured at approximately two orders of magnitude greater than bulk nickel. The temperatures necessary to drive decomposition are also too high for use with paper and plastic substrates.

Li et al.²⁵ reported inkjet printing of conductive nickel lines using a self-reducing reactive ink. The work printed two consecutive streams onto paper at ambient conditions. The first contained 2.5 M aqueous nickel sulfate and the second contained 1.25 M sodium borohydride. Upon mixing, the borohydride ion acted as a reductant for nickel ions to metallize a film. The deposit was confirmed to be metallic nickel with minimal oxidation, but heavily contaminated with sodium-based salts. Li noted that a majority of the salt precipitates atop the deposit, and therefore could be washed off in a post-processing step. Nevertheless, the work reported conductivities 1/600th of bulk metal. While processing at ambient temperature enabled printing on paper, the lack of annealing was likely a major contributor to the poor conductivity.

In another novel approach, Petukhov et al.²⁶ used a two-step process combining inkjet printing and electroless plating to metallize a conductive nickel film. First, a reactive ink containing low concentrations of nickel sulfate and sodium borohydride was printed at 45 °C onto a PEN substrate to seed catalytic nickel particles. Then, the substrate was immersed in an electroless plating bath containing concentrated nickel sulfate and sodium

hypophosphite to metallize the bulk coating. This method produced a thin layer of conductive Ni-P containing 92.5 wt % Ni and 7.4 wt % P. The work demonstrated a unique application of reactive inkjet printing to drastically reduce seeding costs compared to traditional catalysts like palladium nanoparticles and salts.

Ginley et al.²⁷ obtained a patent in 2014 for a high temperature (250 C) self-reducing nickel ink that highly concentrated formate to reduce nickel. Nickel formate was used as the precursor, providing both the nickel ion and the formate ion simultaneously. The salt was dissolved in ethylene glycol along with a small addition of ethylene diamine to enhance solubility. This approach was effective because it concentrated the reagents to simultaneously drive the reduction and produce thick, conductive films. Furthermore, no pH treatment was necessary to maintain deprotonation of the formate as is necessary with use of formic acid. The ink was spray printed onto glass substrates in open atmosphere. XRD confirmed production of metallic nickel without oxides. Further analysis showed lack of organic contamination and near-bulk electrical conductivity. This was a notable feat, as usually reactive inks are an order of magnitude lower, or more. However, the achievement is largely attributed to the high processing temperature, which also makes the ink unviable for printing onto thermally susceptible substrates.

2.4 Electroless Nickel

Two major applications of electroless nickel mechanics are reviewed in this section: plating baths and nanoparticle synthesis. Both are widely practiced in industry and the underlying chemistries have been thoroughly studied.

2.4.1 Plating Baths

Electroless nickel plating baths are a widely used deposition technique for nickel and nickel-alloy coatings. A substrate is activated, via catalyst or surface treatment, and then submerged in a chemical bath. The activated surface catalyzes reduction of free nickel ions which then deposit onto the substrate, steadily building a coating. As a deposition technique, plating baths are capable of cheaply applying even layers to a variety of substrate geometries. Some limitations are that coatings tend to be porous and the baths are often environmentally hazardous.^{28,29}

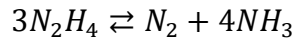
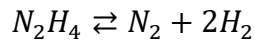
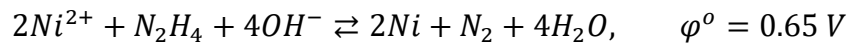
Baths can range from simple to complex, but standard practice is to combine a nickel precursor salt with a reducing agent and a complexing agent in an aqueous bath along with a pH controller to optimize the electrochemical potential of the reductant. Otherwise, additives generally include agents such as accelerators, stabilizers, and more. The additives ensure that nickel only deposits on the substrate and control solution properties, deposition rates, and bath stability.^{28,29}

A variety of reductants are used in EN plating, depending on desired properties. Most common are inorganic complexes of an alkali metal (usually sodium or lithium) and an electron-dense anion like aluminum hydride (AlH_4^-), borohydride (BH_4^-), or hypophosphite (H_2PO_2^-). The nickel is doped with aluminum, boron, or phosphorous, respectively, in each case. Aminoboranes are also frequently used in place of borohydrides to enable a wider range of pH. Common aminoboranes are N-dimethyl amine borane (DMAB) and N-diethylamine borane (DEAB) In cases where pure nickel deposits are desired, hydrazine (N_2H_4) can but these baths are difficult to control; especially at higher temperatures due to decomposition and evaporation.^{28,29}

2.4.2 Nanoparticle Synthesis

Electroless baths for nickel nanoparticle (NiNP) synthesis are currently a major area of research. Many recent works on NiNP synthesis have applied hydrazine as a reductant to synthesize pure nickel nanoparticles.³⁰⁻³⁵ Hydrazine (N_2H_4) is well-known to be a strong, organic reductant. It is highly soluble in water and readily complexes with nickel (II) ions. Moreover, no dopants are deposited in the nanoparticles as with inorganic reductants more commonly applied in plating baths. Thus, it is an ideal reductant for nanoparticle applications where a pure metal is desirable.

Li et al.³⁵ intensively studied the electrochemistry and kinetics of nickel reduction by hydrazine. The following set of reactions was proposed to describe the reduction in basic media:



In which the first reaction describes the primary reduction, and the second two reactions describe decomposition and disproportionation pathways that hydrazine undergoes, catalyzed by nickel.

Li found that the reaction orders are 1, 0, and 1 with respect to nickel (II), hydrazine, and nickel. The latter comes into play since the reduction is autocatalytic; therefore, the kinetics are enhanced with respect to formation of the product. Li also found that the reaction did not proceed at temperature with addition of a small amount of an inducing agent like sodium borohydride or sodium hypophosphite to form initial nucleation sites.

Chandra³⁶ demonstrated that benzyldiethylenetriamine can be an effective reductant for nickel ions in ethanol solvent. However, little other literature could be found referencing this chemical, and it is well-studied compared to hydrazine.

The Polyol Process is an alternative approach to nanoparticle synthesis that reduces metals using high concentrations of weak reductants (polyols) in place of strong reductants like hydrazine. A metal salt is dissolved in a polyol solvent, commonly ethylene glycol, which has a low reducing potential at standard conditions, but a high reducing potential when concentrated at elevated temperatures. This method is mostly used with more-noble metals like gold, silver, platinum, and palladium. However, synthesis of less-noble metals including nickel and cobalt have been reported, where the hydroxides, Ni(OH)₂ and Co(OH)₂ were dissolved and reduced in ethylene glycol. ³⁷⁻³⁹

2.5 Summary

Reactive inkjet printing provides a means to simultaneously synthesize and pattern functional materials. Silver reactive inks have become an established approach to printable electronics on a variety of substrates. Nickel offers a significantly cheaper and nearly as conductive alternative to silver; however, its non-noble chemical characteristic has thus far hindered design of low temperature reactive nickel inks.

Ginley reported the first nickel ink capable of patterning conductive lines with bulk-metal conductivity by utilizing ethylene glycol as a volatile and potent reductant at high temperature. Li and Petukhov showed that strong reductants like borohydride or hypophosphite are capable of reducing nickel salts at temperatures near ambient, at a

sacrifice of product purity. Combining these two approaches, a strong, volatile reducing agent would offer a route to a low temperature, contaminant-free nickel ink.

Recent works in the field of metal nanoparticle synthesis demonstrate hydrazine to be an effective reducing agent for less-noble transition metals like nickel. Moreover, hydrazine, N_2H_4 , is organic and volatile therefore leaving behind no residues post-evaporation. Transitioning the use of hydrazine from nanoparticle synthesis to reactive inks offers a potential solution to developing a low temperature, highly conductive nickel ink.

CHAPTER 3

METHODOLOGY

3.1 Chemicals

Nickel (II) acetate tetrahydrate ($\text{Ni}(\text{OCOCH}_3)_2 \cdot 4\text{H}_2\text{O}$, 98% assay), sodium hypophosphite monohydrate ($\text{NaH}_2\text{PO}_2 \cdot \text{H}_2\text{O}$, $\geq 99\%$ assay), 28 wt % ammonium hydroxide in H_2O (NH_4OH), 1,2-ethanediol ($\text{HOCH}_2\text{CH}_2\text{OH}$), 35 wt % hydrazine in H_2O (N_2H_4), 1,2-propanediol ($\text{CH}_3\text{CH}(\text{OH})\text{CH}_2\text{OH}$), 1,2,3-propanetriol ($\text{HOCH}_2\text{CH}(\text{OH})\text{CH}_2\text{OH}$, $\geq 99.5\%$, 66.0-72.0 wt % ethylamine in H_2O ($\text{CH}_3\text{CH}_2\text{NH}_2$) and 25 wt % tetramethylammonium hydroxide solution in H_2O ($(\text{CH}_3)_4\text{N}(\text{OH})$) were purchased from Sigma-Aldrich (St. Louis, Missouri).

Throughout this work, 28 wt % ammonium hydroxide in H_2O is referred to as ammonia solution, 35 wt % hydrazine in H_2O as hydrazine solution, 66 wt % ethylamine in H_2O as ethylamine solution, 1,2-ethanediol as ethylene glycol, 1,2-propanediol as propylene glycol, 1,2,3-propanetriol as glycerol, and 25 wt % tetramethylammonium hydroxide in H_2O as TMAH.

3.2 Ink Deposition Test Methods

3.2.1 Substrate Preparation

Two substrates were used for tests: glass microscope slides and single-crystal silicon wafer chips. Preliminary pipette tests were carried out on glass slides. Promising samples were reproduced on silicon chips for characterization. Beginning in Chapter 5, samples were sputter coated with 5-10 nm of gold nanoparticles to activate the surface.

3.2.2 Ink Formulation

Ink preparation methods varied throughout the work. The optimal method, investigated and reported in Chapter 7, first mixed the primary and secondary solvents together in a sealed vial. The nickel precursor was dispersed into the mixture and the vial was swirled. After complete dissolution, the base (if applicable) was pipetted into the solution and the vial was again swirled until mixed, which is usually accompanied by a color change. At this point, the solution is very stable. Upon addition of hydrazine, there is potential loss of stability. Therefore, hydrazine was not added until just prior to testing. When time to test, hydrazine solution was pipetted in to complete the ink.

3.2.3 Pipette Testing

The bulk of ink tests reported in this work were deposited by pipetting using micropipettes. In these tests, prepared substrates were heated using a hotplate. Temperature was measured by using Kapton tape to tape down a thermocouple onto the substrate. The Kapton tape acted as a thermally conductive medium to ensure accurate results. Droplets, usually in the range of 20-100 μL , were pipetted onto the substrate once the temperature stabilized.

3.2.4 Printing Tests

Inks were printed with a Nordson Pro4B dispense printer with an Elveflow OB1 pressure controller. Printing on glass used a 27 G nozzle with parameters of 5 mbar pressure, 30 mm/s velocity, and 1 layer. Printing on glass used a 27 G nozzle with parameters of 3 mbar pressure, 30 mm/s velocity, and 2 layers.

3.3 Sealed Vial Test Methods

In sealed vial tests, 10 – 20 mL of ink are reacted within a sealed glass vial, submerged in a water bath to control temperature and magnetically stirred to achieve a well-mixed state. Sealed vial tests provide two advantages versus deposition tests. Firstly, sealed vials provide ideal conditions to isolate thermodynamics of the reaction chemistry by minimizing evaporation to extend the reaction window and allowing for stirring with a magnetic stir rod. By comparison, evaporation and surface tension effects influence the reaction significantly in deposition tests. Secondly, the larger volumes compared to drop-based tests translate to more product for characterization studies like

Inks were mixed with all components except hydrazine, and then placed into a hot, stirred water bath. Temperature and stirring were controlled using ThermoFischer Scientific Cimarec+ hotplates in combination with K-type thermocouples and ... magnetic stir bars. Once the inks were equilibrated with the bath, hydrazine was pipetted in to initiate the reaction. If reaction time was not being controlled, then once the reaction was deemed finished, the vial was removed. In cases where reaction time required control, an acid quench was used to halt the reaction. At the designated time, 1 mL of glacial acetic acid was pipette into the ink, which plummets the pH and catalyzes polymerization of the nickel-hydrazine complex, effectively ‘freezing’ the reaction.

Separation was performed by pipetting the remaining liquid-phase into a centrifuge tube, centrifuging for 1-5 minutes, and then pipetting off the supernatant. Samples were rinsed several times with DI water to remove any remaining residues. Then, samples were either air-dried over several days, or heat-dried overnight in an oven. Once dry, samples were characterized.

Since nickel is magnetic and coats stir bars, the bars had to be cleaned in between each use. Bars were washed in a dilute bath of 5 % aqueous sulfuric acid, by volume. Usually an hour was necessary for all the nickel to dissolve off the bars by visual inspection.

3.4 Product Characterization Methods

A number of characterization techniques were used for characterization including optical microscopy, X-ray diffraction (XRD), scanning electron microscopy (SEM), elemental dispersive X-ray spectroscopy (EDS), and attenuated total reflectance Fourier-transform infrared spectroscopy (ATR-FTIR).

XRD was used primarily for proof of concept studies in which a large sample of product was produced in sealed vial tests. Samples were washed and dried, and then packed onto glass holders to prepare for analysis. Scans were carried out on two sets of equipment. Early proof of concept work, reported in chapter 4, was conducted using a Siemens D5000 powder X-ray diffractometer with a Co-K α tube source. Later work was conducted using a PANalyticalPW3040 X-ray diffractometer with a Cu-K α tube.

SEM and EDS were used in combination for general characterization and to roughly identify the materials and structures present in deposits. Inks were usually deposited onto single-crystal silicon wafers to prepare for SEM. If the materials were suspected to be insulating, an additional coating of gold was sputter coated onto the sample. SEM was conducted using an Amray 1910 field emission scanning electron microscope equipped with an EDAX Octane Series Silicon Drift Detector.

CHAPTER 4

TESTING HYDRAZINE AS A REDUCTANT FOR INKS

4.1 Introduction

Hydrazine (N_2H_4), an organic base, was selected for study because of its ideal vapor pressure (slightly lower than water) and widespread use as a reductant for nickel (II) in nanoparticle synthesis applications (NPS).

In NPS literature, hydrazine is usually combined with a water-soluble nickel salt (e.g. nickel chloride) in strongly basic aqueous media (pH 13 or greater) at slightly elevated temperatures. Basic conditions are provided by alkaline metal-hydroxide salts; most commonly, sodium hydroxide. Under these conditions, reduction is thermodynamically favorable and proceeds on a time scale of minutes to a few hours.

This system can be directly translated into a reactive ink except for the use of alkaline salts, which leave non-volatile inorganic contaminants. From literature³⁵, reduction of nickel by hydrazine is thermodynamically favorable at any pH; however, further increases to basicity continue to enhance the favorability. Hydrazine, being a weak base itself (pK_b of 5.90), can provide considerable basicity, up a pH of 11.2 at 35 wt % in water. Furthermore, there are many weak, volatile bases with lower pK_b 's in the case that hydrazine is insufficient. Examples include ammonia (pK_b of 4.70) and ethylamine (pK_b of 3.20) solutions in water. Thus, it is theoretically possible to design a system that is thermodynamically favorable without the inclusion of a strong inorganic base.

4.2 Proof of Concept: Synthesizing Nickel with Hydrazine Solution

To validate the use of hydrazine, a system based off nanoparticle synthesis literature was studied in sealed vial reactions to produce a sample for XRD analysis. Studying the reaction in a sealed vial models ideal conditions: well-mixed and constant volume with minimal evaporation.

20 mL of solution containing 0.1 M nickel acetate and 2.0 M hydrazine in a 20/80 vol % mixture of ammonia solution and water were combined in a sealed glass vial and vortex mixed to dissolve the nickel. The vial was submerged in a stirred water bath at 60 °C. Owing to the use of ammonia solution, the mixture had a pH around 11 instead of the usual pH of 14 that 1.0 M of NaOH provides.

The solution turned black after about 20 minutes, indicating that the reaction was proceeding. To ensure completion, the vial was kept submerged and heated for 1 hour. Afterwards, the sealed vial was removed, and cooled. A mixture of metallic flakes and solid black precipitant aggregated at the bottom of the remaining mixture of solvents. Additionally, there was a small amount of a white and lilac colored foam suspended in the vial above the liquid phase. An attempt was made to dissolve the foam with solvents including DI water, acetone, and ethanol but the material was insoluble in these so instead the material was scraped out. The vial was heated while open to atmosphere to drive off remaining solvent, and then the solid precipitants were transferred to a slide for XRD analysis, shown in Figure 1. All expected nickel peaks were present in the spectrum, confirming that metallic nickel was synthesized and thereby validating the hydrazine approach.

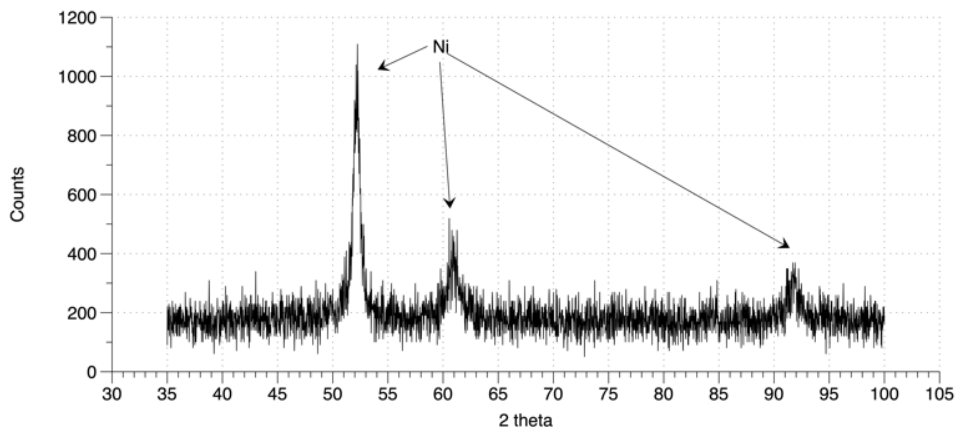


Figure 1. XRD pattern of nickel sample synthesized using hydrazine as a reductant at 60 °C in a 20/80 vol % mixture of water and ammonia solution. Reference peaks for nickel using Co-K α radiation are 32.01°, 60.81°, and 91.38° with relative peak intensities of 100, 50, and 40, respectively.

4.3 Preliminary pipette Tests with Hydrazine

In a sealed vial setting, hydrazine proved a capable reductant for nickel. Next, the formulations of 0.1 and 0.25 M nickel acetate with 2.0 M hydrazine in a 20/80 vol % mixture of ammonia solution and water were pipetted onto glass slides at temperatures ranging from ambient to 100 °C. In all tests, a flaky lilac material precipitated instead of metal, as shown in Figure 2.

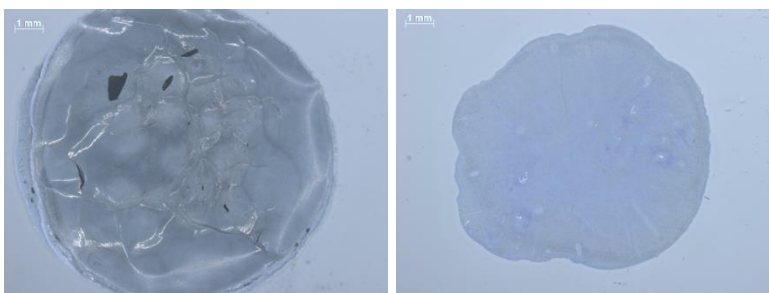


Figure 2. Optical image of hydrazine-based ink containing (a) 0.25 M [Ni²⁺]; (b) 0.1 M [Ni²⁺], 2.0 M [N₂H₄] and 12.3 M [NH₃] in DI water, pipetted onto a glass slide at 60 °C.

4.4 Testing Approaches to Facilitating Reduction

The nickel-hydrazine system was demonstrated effective in a large-volume setting where component evaporation and reaction time are insignificant factors, but when these effects came to play in a droplet, the system failed to metallize. A number of approaches were tested to address these effects including varying concentrations, using higher boiling solvents to lower vapor pressure, and initiating the reaction via catalysts and inductants.

4.4.1 Varying Nickel and Hydrazine Concentrations

Nickel acetate concentration was varied between 0.025 and 1.0 M. The salt stopped dissolving well at concentrations past about 0.25 M. Lower amounts produced smoother deposits (Figure 2a) while higher amounts caused thick, porous deposits (Figure 2b).

Hydrazine concentration was varied between 1 and 5 M. Higher concentrations produced more bubbling and less smooth films but did not seem to affect material nature.

4.4.2 Testing Alternative Solvents

Two categories of solvents were investigated. The first (column 1) characteristically have lower vapor pressure than water. These were studied assuming that inks were not metallizing because the solvent was evaporating quickly. The second category (column 2) studied some unique functional groups to screen whether it had an effect on the system.

Ethylene glycol	Ammonia Solution
Diethylene glycol	Methanol
Glycerol	Ethanol
2,3-butanediol	Ethylamine

The same base formulation of 0.1 M nickel acetate and 2.0 M hydrazine was mixed into each of the solvents separately for study. The inks were pipetted onto glass slides at temperatures ranging from ambient to 100 °C. In all cases, one of three results occurred:

- Reprecipitated the nickel acetate salt (Figure 3a)
- Produced a powdery lilac material (Figure 3b)
- Produced a porous white material (Figure 3c)

Ultimately, changing the solvent failed to facilitate reduction in these tests, indicating solvent effects were not the primary issue preventing reduction.



Figure 3. Common products of nickel reactive inks containing nickel acetate, hydrazine, ammonia, water, and simple alcohol or amine-based solvents. (a) green salt; (b) porous white material; (c) purple salt.

4.4.3 Testing Palladium Chloride as a Solution-Phase Catalyst

In electroless nickel plating applications, it is common to use a catalyst to direct reduction and overcome the stabilizing effect that strong complexing agents have on nickel ions in solution. An attempt was made to add palladium chloride into the aforementioned ink mixtures to catalyze the initial formation of nucleation sites. Addition to inks sometimes resulted in a metallized layer, visible through the underside of the glass slide, but did not cause the bulk of the droplets to reduce.

4.4.4 Hypophosphite as a Solution-Phase Inducing Agent

Li³⁵ reported using a minute addition of sodium borohydride as an inducing agent in place of a catalyst. This approach takes advantage the autocatalytic nature of nickel, with respect to its electrochemical reduction. The borohydride ion is a potent reductant for nickel and does not require catalyst if the complexing agent is weak to moderate strength (e.g. water or ammonia). A small addition of sodium borohydride produces nanoparticles dispersed throughout the solution, which in turn act autocatalytically to initiate the bulk hydrazine reduction reaction.

To attempt this approach, sodium hypophosphite was used in place of borohydride. The two are very similar in terms of reduction potential and solubility. In sealed vial tests, inks were mixed together without hydrazine at temperatures between 30 - 60 °C. Sodium hypophosphite was added in mass ratios ranging from 5-10 mg NaH₂PO₂ per 100 mg Ni(CH₃CO₂)₂. Mixtures were left alone for 5-15 minutes to allow hypophosphite ions to produce nucleation sites. Then, hydrazine was added to initiate the bulk reaction.

Results were mixed; in some cases, addition of the hypophosphite seemed to speed up the reaction, but this observation was inconsistent. There was little discernable effect on the upper layers of the final products but the lower layers of the deposit clearly metallized (Figure 4). Notably, the upper layers of the failed in the same manner as without addition of inductant.

Even minute amounts of inductant produced visible sodium contamination of the surface of deposits. Taking into account the inherent inorganic nature of most potential inductants contamination is inevitable; thus, use of inductants is non-ideal.

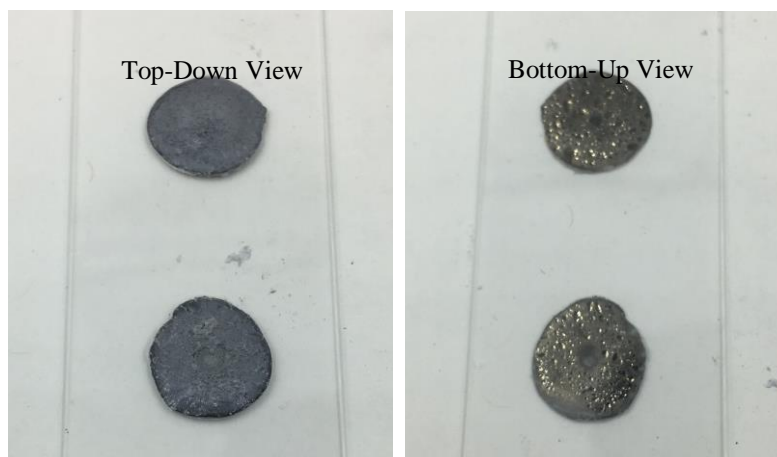


Figure 4. Top and bottom views of deposit produced by pipetting water-based ink containing 0.1 M $[\text{Ni}^{2+}]$, 2.0 M $[\text{N}_2\text{H}_4]$, and 0.016 M $[\text{NaH}_2\text{PO}_2]$ onto a glass slide at 60 °C.

4.5 Summary

Hydrazine proved to be an effective reductant for nickel acetate under ideal condition but preliminary work to translate the nickel-hydrazine system into pipette tests failed to produce metal product. Varying agent concentrations and solvents affected the general appearance of deposits (e.g. shape, topology) but did not lead to metallization. Various approaches were taken to favor reduction, but none showed significant success except for addition of inductant, which produced a metallic lower layer and seemed to be a step in the right direction.

CHAPTER 5

HIGH TEMPERATURE GLYCEROL-SOLVATED INKS

5.1 Introduction

The previous section demonstrated that under ideal conditions in a sealed vessel, hydrazine is a potent reductant for electrochemical synthesis of nickel. When pipetted as a droplet, the same formulations fail to reduce; instead, generating various undesired products. It was theorized that a misbalance of reduction and droplet evaporation kinetics were causing nickel salts to reprecipitate prior to completion of the reaction.

The proposed solution was twofold: addition of catalyst to initiate reduction and integration of polyol solvents to lower the bulk vapor pressure, thereby increasing the reaction window. To catalyze reactions, gold nanoparticles were sputter coated onto substrates. To lower vapor pressure, polyols including ethylene glycol (EG), propylene glycol (PG), and glycerol were considered.

5.2 Screening Polyols

Three inks were formulated with different solvents (EG, PG, and glycerol) and then pipetted at either 100 °C for EG and PG, or 150 °C for glycerol to account for volatility.

Without a catalytic surface coating the inks did not reduce, as shown in Figure 5. The resultant ink deposit varied significantly according to the polyol. In ethylene glycol, a green precipitant resembling the hydrated nickel acetate salt formed. In propylene glycol, a combination of purple and white precipitants formed. In glycerol, the deposit appeared to be a green-brown salt encased in clear residue.

When the substrates were treated with a gold coating, results changed dramatically as shown in Figure 6. Instead of reprecipitating colored salts, metallization was observed. In the case of ethylene and propylene glycol, a metal layer deposited out of solution within about 30 seconds, but as the rest of the solvent dried the metal layer was coated in white material. This is especially visible in the propylene glycol sample. In the case of glycerol, pipetted at 150 °C, the ink appeared to fully reduce into a patchy deposit of metal. From these results, it was decided to use glycerol for further high temperature inks.



Figure 5. Dried droplets of ink pipetted onto untreated glass. Formulation was 0.1 M nickel acetate and 2 M hydrazine in a 20/80 vol % mixture of ammonia solution and polyol. Solvent and deposition temperatures are: (a) ethylene glycol, 100 °C; (b) propylene glycol, 100 °C; (c) glycerol, 150 °C.

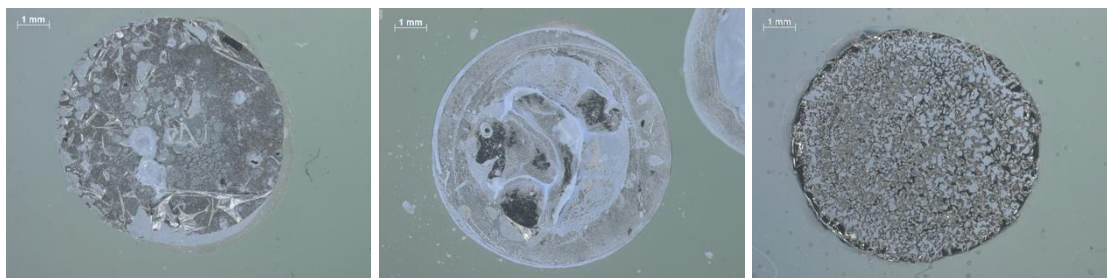


Figure 6. Dried droplets of ink pipetted onto gold-coated glass. Formulation was 0.1 M nickel acetate and 2 M hydrazine in a 20/80 vol % mixture of ammonia solution and polyol. Solvent and deposition temperatures are: (a) ethylene glycol, 100 °C; (b) propylene glycol, 100 °C; (c) glycerol, 150 °C.

5.3 Glycerol-Solvated Inks

Many glycerol-solvated inks were synthesized during this portion of the work. Nickel acetate concentration was varied from 0.025 – 0.5 M before narrowing the range to 0.05-0.1 M because its solubility is low in glycerol. Hydrazine molar ratio, with respect to nickel, was varied from 5 to 50. The ratio had less of an effect than expected; if the ratio was maintained above 5, the factor did not seem to affect deposition rates or nature of the final product. Bubbling increased with hydrazine concentration so that when $[N_2H_4]$ rose above about 4.0 M, bubbles noticeably damaged the surface of the deposits. Ammonia concentration was varied from about 0.5-5 M. At high concentrations, droplets evaporated quickly and bubbled violently, destroying the deposits. Inks were also tested without ammonia entirely; from visual inspection, this did not seem to influence the final product, suggesting that hydrazine is sufficiently basic, itself. This is supported by how the hydrazine and ammonia have relatively close pK_b 's in water.

Figures 7 and 8 show optical microscopy and SEM for a representative deposit produced by glycerol-based inks. In this case, the composition was 0.05 M $[Ni^{2+}]$, 1.8 M and $[N_2H_4]$ in glycerol and the ink was pipetted onto gold-coated glass at 150 °C.

Optical microscopy (Figure 7) shows what appears to be a metallic deposit with a film coating it. The lack of shine was attributed to the formation of nanoparticle clusters and, potentially, oxides. Some charging in the SEM (Figure 8) supported these observations, although the use of glass as the substrate also contributed to charging. The surface of the deposit appeared cracked and flaked. It was difficult to discern the nature of the materials from microscopy alone.

EDS (Table 1) confirmed a significant carbon and oxygen presence. It is important to note that since the spectroscopy was carried out on a glass slide, the substrate contributed partially to the oxygen content. Together, the remaining oxygen and the significant carbon present two sources of contamination: nickel oxides, unreduced nickel acetate, and a polymer formed by glycerol, likely catalyzed by synthesized nickel.

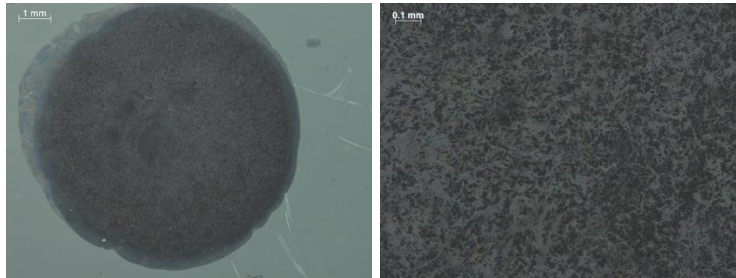


Figure 7. Optical images of deposit produced by pipetting a glycerol-based ink containing 0.05 M $[\text{Ni}^{2+}]$ and 1.8 M and $[\text{N}_2\text{H}_4]$ at 150 °C onto a gold-coated glass slide.

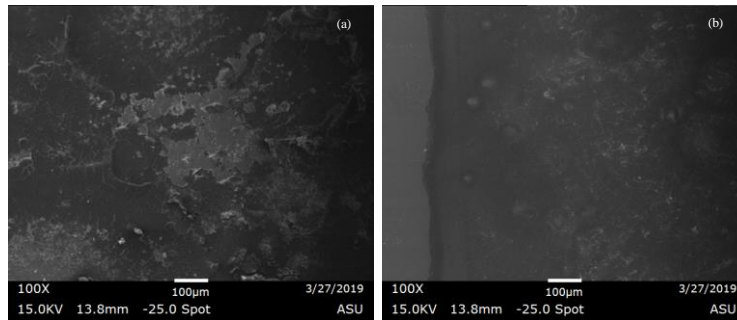


Figure 8. SEM of deposit produced by pipetting a glycerol-based ink containing 0.05 M $[\text{Ni}^{2+}]$ and 1.8 M and $[\text{N}_2\text{H}_4]$ at 150 °C onto a gold-coated glass slide.

Table 1. EDS elemental weight and atomic distributions in deposit produced by pipetting a glycerol-based ink containing 0.05 M $[\text{Ni}^{2+}]$ and 1.8 M and $[\text{N}_2\text{H}_4]$ at 150 °C onto a gold-coated glass slide.

<i>Element</i>	<i>Weight %</i>	<i>Atomic %</i>
<i>Ni</i>	71	37
<i>C</i>	12	31
<i>O</i>	17	32

5.4 Glycerol-Solvated Inks with Addition of an Inductant

Solvation in glycerol seemed to facilitate reduction by lowering the bulk vapor temperature to allow for higher temperatures. However, the temperatures were too high to meet the objectives of the project. In an attempt to lower the reaction temperature by speeding up the kinetics, the inducing agent approach from Section 4.4.4 was revisited.

To test the effects of inductant, an ink composed of 0.1 M $\text{Ni}(\text{CH}_3\text{CO}_2)_2$, 3.5 M N_2H_4 , and 0.015 M NaH_2PO_2 in a 30/70 vol % mixture of DI water and glycerol was pipetted onto gold-coated glass at 125 °C. To the eye, the resultant spot appeared metallic with some residue. The deposit had a dark green tinge, consistent with some nickel oxides. Optical microscopy (Figure 9) showed large crystals embedded at the center.

The deposit on the gold-coated glass slide was analyzed with SEM, shown in Figure 10. Significant charging occurred during SEM; possibly a result of the glass substrate and the presence of salts and oxides in the deposit. Figure 11 confirmed the presence of large crystals near the center. The crystals appeared to move due to charging, indicating them to be a salt. Additionally, salt ring was observed at the boundary region (Figure 10b); likely produced by the coffee-ring effect transporting sodium salts as the droplet dried.

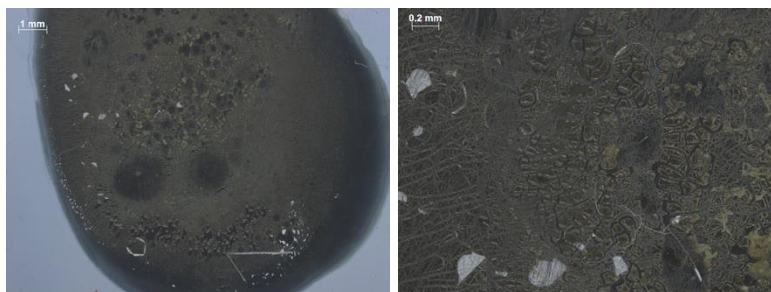


Figure 9. Images of deposit produced by pipetting glycerol-solvated ink containing 0.1 M $[\text{Ni}^{2+}]$, 3.6 M $[\text{N}_2\text{H}_4]$, and 0.015 M $[\text{NaH}_2\text{PO}_2]$ onto gold-coated glass at 125 °C.

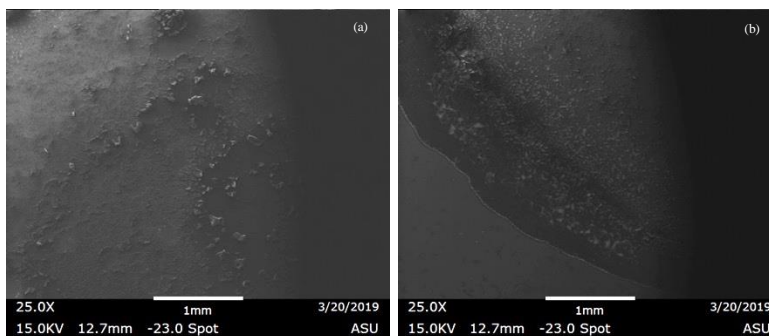


Figure 10. SEM of deposit produced by pipetting glycerol-solvated ink containing 0.1 M $[\text{Ni}^{2+}]$, 3.6 M $[\text{N}_2\text{H}_4]$, and 0.015 M $[\text{NaH}_2\text{PO}_2]$ onto gold-coated glass at 125 °C. (a) bulk region; (b) boundary region.

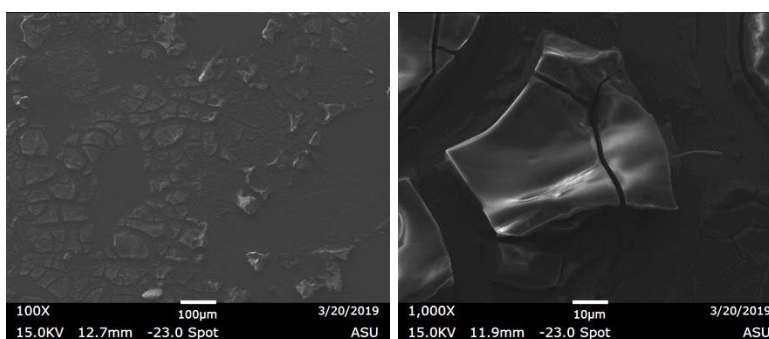


Figure 11. SEM of crystals embedded on deposit produced by pipetting glycerol-solvated ink containing 0.1 M $[\text{Ni}^{2+}]$, 3.6 M $[\text{N}_2\text{H}_4]$, and 0.015 M $[\text{NaH}_2\text{PO}_2]$ onto gold-coated glass at 125 °C.

EDS (Table 2) was carried out on the sample, but since the ink was deposited onto glass it was not possible to differentiate whether oxygen was sourced from the ink deposit or the glass substrate. In accordance, EDS results are presented as two separate scans. The first scanned for Ni, Na, P, C, O, and Si while the second excluded Si and O to isolate the deposit. FTIR (Figure 12) was also conducted to identify notable organic stretches. In this case, background from the substrate was accounted for.

FTIR and EDS confirmed the presence of organics. The second EDS scan (carbon, nickel, and sodium) measured a carbon atomic percentage of 36.55 which is too significant to attribute to residue. Formation of sodium acetate is a possible source of the

carbon retention; however, there is no carboxylic acid peak in FTIR. The only common peak identifiable from FTIR is an O-H stretch between 3500 and 3000 cm^{-1} . This O-H stretch would be consistent with formation of a polyol-based polymer, however expected alkyl C-H stretches for such a compound are also missing. Ultimately, it was difficult to discern specifics from FTIR, but the results did confirm formation of a residue.

Table 2. EDS-sourced elemental composition of the deposit produced with a glycerol-based ink containing inductant at 125 °C.

<i>Element</i>	<i>EDS Scan 1</i>		<i>EDS Scan 2</i>	
	<i>Weight %</i>	<i>Atomic %</i>	<i>Weight %</i>	<i>Atomic %</i>
<i>Ni</i>	55	27	70	41
<i>Na</i>	6	7	8	12
<i>P</i>	8	7	20	11
<i>C</i>	9	22	13	37
<i>O</i>	18	32	-	-
<i>Si</i>	4	4	-	-

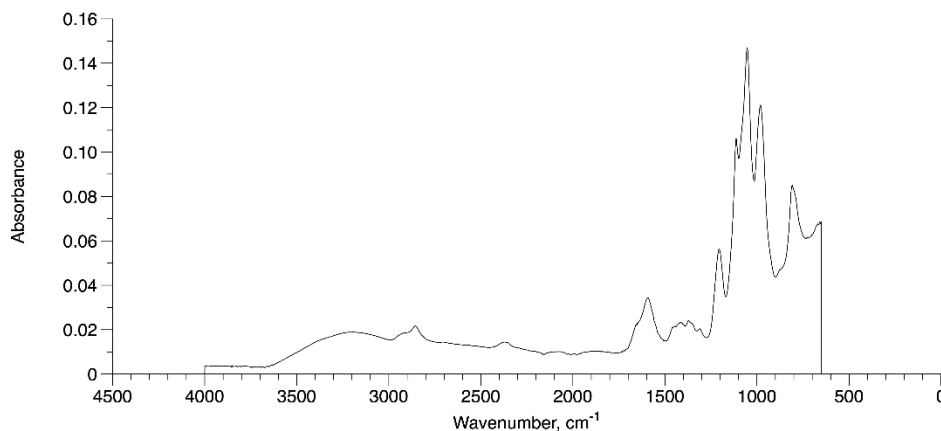


Figure 12. FTIR of deposit produced by pipetting glycerol-solvated ink containing 0.1 M $\text{Ni}(\text{CH}_3\text{CO}_2)_2$, 3.5 M N_2H_4 , and 0.015 M NaH_2PO_2 onto gold-coated glass at 125 °C.

5.5 Summary

Chapter 5 investigated enhancing the reduction reaction via high temperature, surface activation, and addition of inductant. These approaches resulted in the first signs of fully metallized product (Figure 6). Upon closer inspection, microscopy, SEM and EDS identified the presence of residues, oxides, and, when inductant was added, sodium salts.

The carbon residues were attributed to the use of polyols as solvents, as the group of chemicals tends to be susceptible to polymerization. Nickel nanoparticles in the ink would only enhance this phenomenon through catalysis.

The significant oxygen content observed in EDS was attributed to the formation of nickel oxides, which was in turn hypothesized to be a result of depositing the inks at high temperatures in ambient air. In the future, using inert atmospheres would present a route to preventing oxidation.

Sodium salts were an expected result of the use of sodium hypophosphite as an inductant. The coffee-stain effect carried some of the sodium to the boundary, resulting in a purer bulk region. Nevertheless, sodium contributed 7.88 wt % to the bulk deposit according to EDS, which would be highly detrimental to electrical conductivity.

Ultimately, the work in this chapter served to validate that metallization via pipetting droplets is possible; however, an optimal ink should deposit at much lower temperatures and be void contamination. Moving forward, it was necessary identify creative routes to facilitate reduction at lower temperature ranges.

CHAPTER 6

TRANSITIONING TO LOW TEMPERATURE INKS

6.1 Introduction

Chapter 5 introduced some nickel reactive inks that reduce at high temperatures in glycerol to produce semi-metallic deposits. From FTIR and EDS, there was a significant organic presence. Moreover, the high temperatures seemed to oxidize the nickel. Chapter 6 aims to investigate routes to lower the deposition temperature below 100 °C and reducing organic contamination to no more than 10 wt %.

Firstly, some low temperature solvents were screened to identify a replacement for glycerol. Afterwards, several studies conducted to better understand the chemistry of the system are covered. This includes identifying sources and conditions for the formation of various complexes and products frequently observed as well as factors driving reduction. Lastly, some early attempts at low temperature inks are reported, based off of the solvent screening and the results from the chemistry studies.

6.2 Screening Low Temperature Solvents

Three alternatives to glycerol were considered including ammonia solution, propylene glycol, and ethylene glycol. Ammonia solution, boiling point 37.3 °C, is commonly used in silver reactive inks and solvates nickel acetate exceptionally well. Propylene glycol is chemically and structurally similar to glycerol but boils at 188.2 °C. Ethylene glycol has a similar boiling point to propylene glycol at 197.3 °C but is chemically more active.

6.2.1 Ammonia-Solvated Inks

Two ammonia-based formulations were studied varying the concentration of nickel acetate between 0.05 and 0.10 M $[\text{Ni}^{2+}]$. Otherwise, the composition was 1.5 M $[\text{N}_2\text{H}_4]$ in 16.7 vol % water and 83.3 vol % ammonia solution.

Nickel concentration was a parameter of interest here because nickel solubility was a major limitation of polyol-based inks. Poor solubility was hypothesized to be a cause of salt reprecipitation as solvents evaporated. It was hoped that the considerable solubility of nickel acetate in ammonia solution would enable more concentrated inks, leading to enhanced kinetics and thicker deposits of metal.

The formulations were pipetted onto gold-coated glass slides at four temperatures each. Pure ammonia solution boils at 37.3 °C and makes up the majority of the ink. Boiling point elevation increases this marginally, but nevertheless the low boiling point constrains the ink to low temperature deposition. Thus, chosen temperatures for study were 35, 45, 55, and 70 °C.

The low viscosity of ammonia solution complicated the deposition process. Ink began to drip out of the pipette tips immediately after loading, hindering precise control of pipetted volume. Furthermore, after pipetting the ink wet the surface resulting in a wide and irregularly-shaped spot instead of a reproducible and symmetric droplet, as with more viscous solvents. Lastly, as the ammonia evaporated the droplet slid around the surface of the substrate, eventually leaving behind a concentrated droplet of hydrazine solution and nickel acetate. This phenomenon is a consequence of the disparity in boiling point between hydrazine solution and ammonia solution (114 and 37.3 °C, respectively).

Figures 13 and 14 show images of the deposits at several temperatures.

Observation yielded a few key info. The visual lack of metallic product on either the top or bottom of the deposit suggested that the inks were not capable of reduction. In the lower concentration (0.05 M) samples, there is not a visible salt precipitant but there is thin-film interference can be soon. In the higher nickel concentration (0.10 M) samples, there was clearly a non-metallic precipitant. The color varied with temperature; lilac at 45 °C and white at 70 °C, indicating formation of a temperature-sensitive complex. It was hypothesized that the precipitant was a result of the enhanced nickel concentration driving complexation and possibly polymerization with hydrazine.

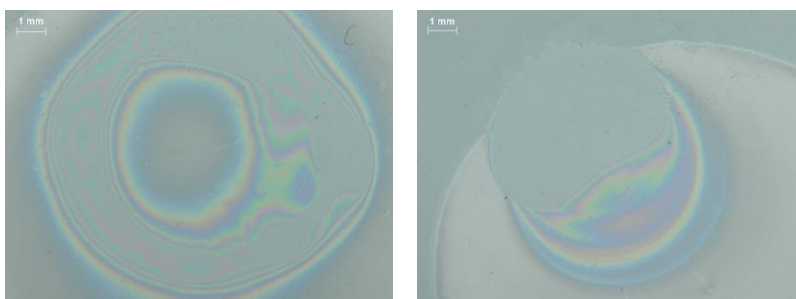


Figure 13. Optical images of deposits produced by pipetting an NH_3 -based ink (0.05 M $[\text{Ni}^{2+}]$, 1.8 M $[\text{N}_2\text{H}_4]$, and 12.3 M $[\text{NH}_3]$ in water) onto gold-coated glass microscope slides at (a) 35 °C and (b) 45 °C.

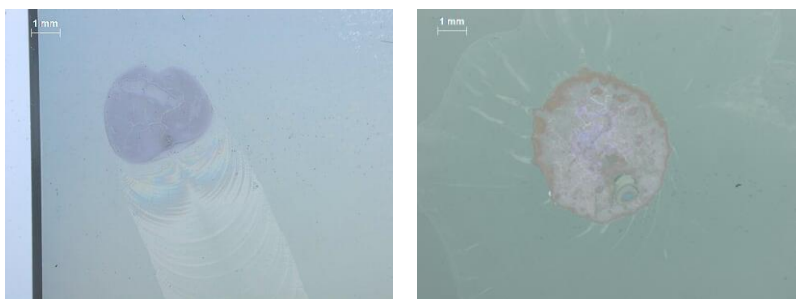


Figure 14. Optical images of deposits produced by pipetting an NH_3 -based ink (0.10 M $[\text{Ni}^{2+}]$, 1.8 M $[\text{N}_2\text{H}_4]$, and 12.3 M $[\text{NH}_3]$ in water) onto gold-coated glass microscope slides at (a) 45 °C and (b) 70 °C.

6.2.2 Propylene Glycol-based Inks

Propylene glycol (PG) was studied with one ink, which replaced glycerol with PG in the inks reported in Chapter 5. The formulation was 0.05 M $[\text{Ni}^{2+}]$ and 1.8 M $[\text{N}_2\text{H}_4]$ in 16.7 vol % water and 83.3 vol % PG. The ink was pipetted at four temperatures from 60 to 90 °C. At 60 °C droplets took a significant amount of time to dry. At 90 °C the droplets dried in about 15-20 minutes. Owing to moderate viscosity and minimal wetting, PG proved to be a good bulk solvent for pipetting reproducible droplets. Figure 15 provides optical images of PG-based ink deposits at 60 and 90 °C.

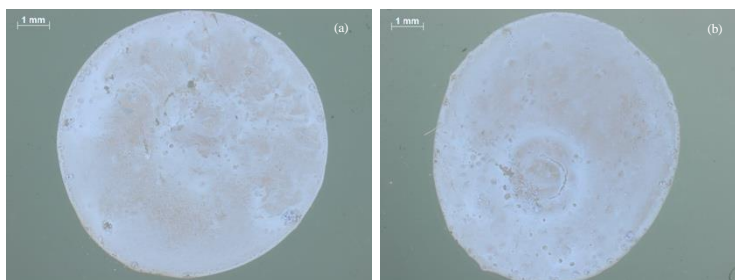


Figure 15. Optical images of PG-based ink (0.05 M $[\text{Ni}^{2+}]$ and 1.5 M $[\text{N}_2\text{H}_4]$ in 33.3 vol % DI water and 66.7 vol % PG). Droplets were pipetted onto gold-coated glass. Results shown for (a) 80 °C and (b) 100 °C.

From visual observation, the ink rapidly reduced an initial layer, and then an opaque material deposited well before the glycol finished evaporation. Once dried, the material was white. It was similar to what was seen in the NH_3 -based inks at higher temperatures.

Since PG is chemically similar to glycerol, the prime difference between this ink and the glycerol inks is processing temperature; 60-100 °C for PG and 115-200 °C for glycerol. These results indicated that the higher temperature range employed in glycerol inks is necessary for the hydrazine to be capable of reducing nickel.

6.2.3 Ethylene Glycol-based Inks

Ethylene glycol (EG) was studied with one ink, which replaced glycerol with ethylene glycol in the inks from Chapter 5. The formulation was 0.05 M $[\text{Ni}^{2+}]$ and 1.8 M $[\text{N}_2\text{H}_4]$ in 16.7 vol % water and 83.3 vol % propylene glycol. The ink was pipetted 80 and 100 °C. Figure 16 shows corresponding optical images.

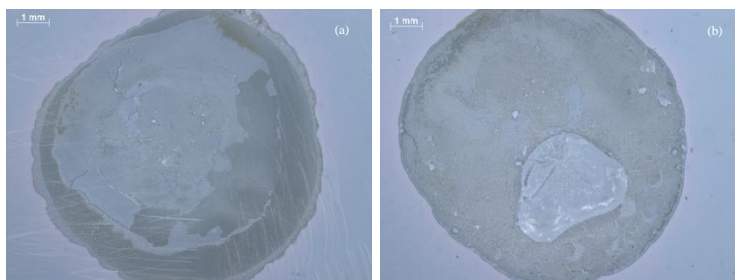


Figure 16. Optical images of EG-based ink (0.05 M $[\text{Ni}^{2+}]$ and 1.5 M $[\text{N}_2\text{H}_4]$ in 16.7 vol % DI water and 83.3 vol % PG). Droplets were pipetted onto gold-coated glass. Results shown for (a) 80 °C and (b) 100 °C.

As with the PG-based ink, the EG-based ink rapidly reduced an initial layer of metal, but then formed a white material on top. These results further supported that temperatures well above 100 °C are necessary to reduce nickel under these conditions.

6.2.4 Results of Solvent Screening

The short study on ammonia solution demonstrated that at this stage it is not viable as the bulk solvent. Inks using it produced unpredictable nickel-based materials, in irregularly-shaped deposits. PG and EG were a little more promising; the deposits were more reproducible, and metal was observed in the bottom layers by looking through the underside of the glass slides. However, a white material, hypothesized to be a nickel-hydrazine complex was repeatedly, forming in the upper layers of the deposit.

6.3 Chemistry Studies

The appearance of many new materials in low temperature inks suggested that the chemistry space was not well understood. To better understand what materials were forming and why, several chemistry-focused studies were conducted.

First, the white material was characterized using SEM and EDS. Then, the solution-phase complexes that form during ink synthesis were examined. Lastly, the effects of pH were visited in case the previous assumption that hydrazine provides sufficient hydroxide concentration was actually false.

6.3.1 Identifying the White Material

The propylene glycol ink synthesized in Section 6.2.2 was reproduced onto gold-coated silicon for analysis with SEM and EDS. Optical microscopy (Figure 17), confirmed reproduction and reiterated that the material was flaky, porous, and clearly non-metallic. SEM further showed that the material was a series of porous platelets in the bulk regions (Figure 18) and spongy in the boundary (Figure 19).

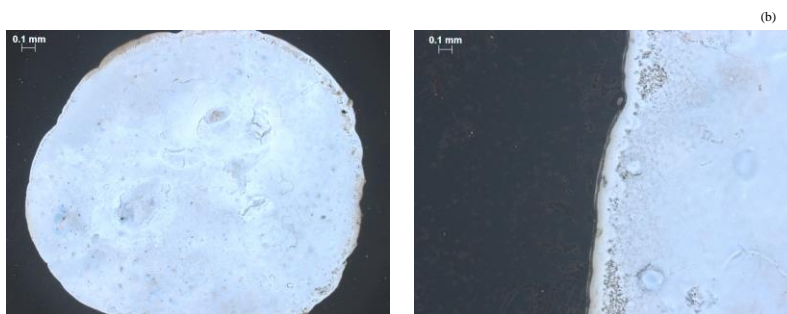


Figure 17. Optical imagery of the bulk white material. The deposit was synthesized by pipetting an ink composed of 0.05 M $[\text{Ni}^{2+}]$ and 1.5 M $[\text{N}_2\text{H}_4]$ in 16.7 vol % DI water and 83.3 vol % PG onto gold-coated silicon at 75 °C.

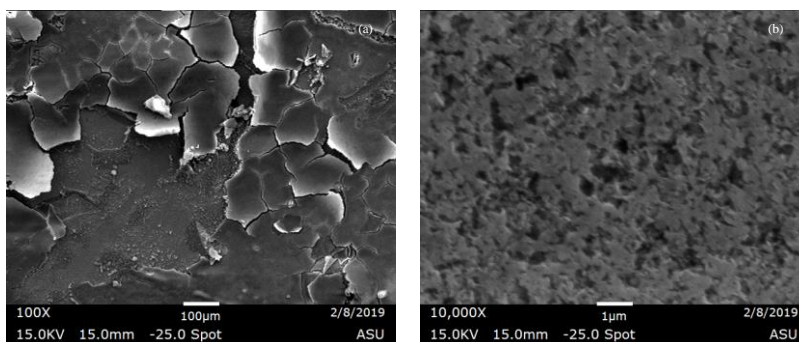


Figure 18. SEM of the bulk regions of the white material. Deposit produced from PG-based ink pipetted on silicon at 75 °C.

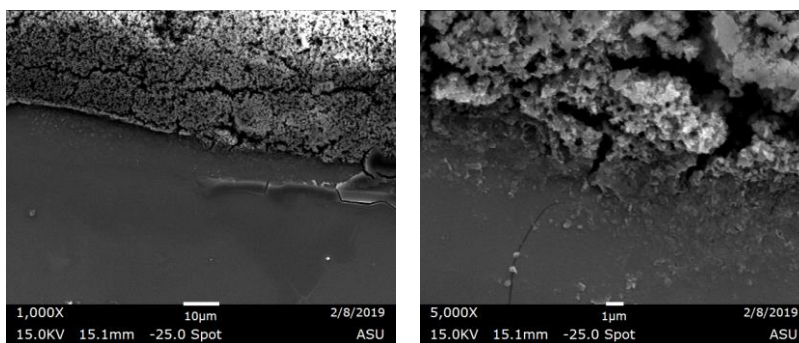


Figure 19. SEM of the boundary region of the white material. Deposit produced from PG-based ink pipetted on silicon at 75 °C.

From EDS analysis (Table 3), there are four major elements present in the sample: nickel, carbon, nitrogen, and oxygen. Carbon and oxygen are provided by both the acetate ion and the glycol. The only precursor for nitrogen in the ink was hydrazine, indicating that some undesired reaction was occurring to retain nitrogen from the hydrazine. Taking into account the three contaminants forming (carbon, nitrogen, and oxygen), the results pointed to the formation of a thermally stable metal-organic complex; otherwise the heat should decompose or evaporate the organics (hydrazine, ammonia, acetic acid, propylene glycol).

Table 3. Atomic and weight distributions of the white material determined by EDS. Deposit produced from PG-based ink pipetted on silicon at 75 °C.

<i>Element</i>	<i>Weight %</i>	<i>Atomic %</i>
<i>Ni</i>	62	28
<i>C</i>	14	31
<i>N</i>	10	18
<i>O</i>	14	24

6.3.2 Isolating the Source of Lilac-Colored Complex and Precipitant

Something commonly observed in tests using polyols as solvents was the formation of a lilac complex in synthesized inks, followed by clouding of the ink and then precipitation of a lilac material. The sporadic appearance of the lilac precipitant prompted an investigation to identify the source. 75 mg of nickel acetate was dissolved separately into 3 mL of each liquid commonly used, as well as under different pH conditions. The resultant complex was recorded. Table 4 reports the results.

The complex was first seen in the study when 0.1 M nickel acetate was dissolved in hydrazine solution under acidic conditions. Prior to addition of acid, the solution was light purple. Immediately after addition of acid, a white-lilac material precipitated out.

Another test was conducted in which 0.5 M nickel acetate was dissolved in hydrazine solution. The mixture had trouble fully dissolving and was shaken to speed up dissolution. Immediately upon shaking, the solution began to precipitate out the lilac material (Figure 20). After further study it was found to form without shaking as well, but at a slower rate.

Table 4. Complexes Formed by Mixing 0.1 M Nickel Acetate Tetrahydrate in Common Solvents at Ambient Conditions.

<i>Solvent</i>	<i>Color</i>	<i>Solubility</i>
<i>DI water</i>	Green ¹	Moderate
<i>DI water, pH 2</i>	Green ¹	Poor
<i>DI water, pH 13</i>	Light blue-green	Moderate
<i>28 wt % ammonia sol.</i>	Violet	Excellent
<i>35 wt % hydrazine sol.</i>	Light purple to lilac	Moderate
<i>Polyol (EG, PG, Glycerol)</i>	Green ¹	Poor, decreasing with molar mass
<i>35 wt % hydrazine + acetic acid</i>	Lilac-white blend ³	insoluble
<i>35 wt % hydrazine + 0.4 M NaOH</i>	Royal blue	Good

¹ Same green color as the base nickel acetate tetrahydrate salt.
² Thick foamy lilac-white material that precipitated out of solution.

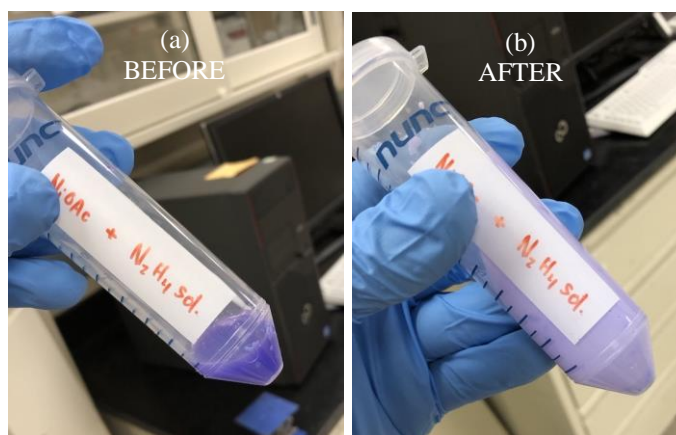


Figure 20. 0.5 M nickel acetate tetrahydrate in 35 wt % hydrazine solution in water, before and after lightly shaking, showing what is hypothesized to be a polymerization reaction of a nickel-hydrazine complex.

Nickel acetate solvated in water forms a green complex. Addition of hydrazine causes an immediate transition to a purple solution (Figure 20a), confirming formation of a stable nickel-hydrazine complex. When the nickel acetate is concentrated enough a second transition occurs to precipitate an insoluble lilac material (Figure 20b).

Considering the factors affecting production of the material, a likely explanation is polymerization. Gustafsson et al.⁴⁰ reported characterization of a nickel (II) complex including hydrazine, sulfato, and hydroxo bridging that form trimers and hexamers, demonstrating that can act as a bridging ligand to polymerize nickel (II) complexes. Furthermore, formation of such a large molecule would explain the stabilization and subsequent precipitation from solution.

Assuming that the precipitant is in fact a polymer, then the polymerization is a competing reaction with the desired reduction. Therefore, future work must account for this potential reaction, by designing inks and deposition conditions to emphasize the reduction reaction and block polymerization.

6.3.3 Effects of pH on the System

The complex study (Table 4) revealed that pH conditions affect how nickel and hydrazine complex. Nickel acetate dissolved purely in hydrazine solution formed a violet solution. Addition of acid induced precipitation of the lilac precipitant, while addition of base transformed the solution to a royal blue color. In Ni nanoparticle (NiNP) literature, sodium hydroxide is employed in excess concentrations as high as 1.0 M to ensure that pH stays constant near 14 and there is sufficient hydroxide for the reduction reaction. Also, NiNP literature never reports observation of the lilac precipitant. Taking all these

observations into account, it was hypothesized that basic conditions play a role in stabilizing the nickel-hydrazine complex as a monomer.

To test this theory, a sample of polymer was synthesized in a centrifuge tube by precipitation of 5 mL of 0.5 M nickel acetate in hydrazine solution. Then, 5 mL of 0.4 M NaOH in water were added to the tube. Almost instantaneously, the polymer redissolved, forming a royal blue solution. An additional 0.5 g of nickel acetate were added, and then the solution was left alone at ambient conditions for one week. After this period no visual changes were observed, and no precipitant could be seen.

Altogether, these results indicated that maintaining a $\text{pH} > 13$ is a critical parameter to ensure stabilization of the solution and supply of hydroxide for the reduction.

6.3.4 Ink Mixing Order

Based on the results from the complexing study it was decided that mixing order should be a controlled parameter to ensure that the ink is properly and reproducibly synthesized, as well as to avoid polymerization.

From observation of past experiments, the nickel acetate dissolved best when a good solvent was added first, which makes intuitive sense. A standard ink composed of 0.1 M $[\text{Ni}^{2+}]$ and 1.5 M N_2H_4 in 50 wt % H_2O and 50 wt % PG was mixed into glass vials in three separate orders:

- Nickel acetate, DI water, propylene glycol, hydrazine solution
- Nickel acetate, propylene glycol, DI water, hydrazine solution
- Nickel acetate, hydrazine solution, propylene glycol, DI water

The first route performed best; nickel partially dissolved in the water, diluted with addition of PG, and then fully dissolved with addition of hydrazine solution. The second route struggled to dissolve the nickel, which clumped in the sole presence of the glycol, but eventually the majority of the salt dissolved. The third route began as a transparent purple solution upon addition of hydrazine solution but rapidly transitioned to a cloudy lilac as material precipitated out upon swirling the vial. Addition of the other solvents did not redissolve the polymer.

These results indicated that to maintain ink stability hydrazine should be added at the end, once the nickel acetate is fully dissolved in other solvents. This makes intuitive sense after the previous sections demonstrated that the lilac precipitant is a result of a side reaction between nickel and hydrazine; inks should be formulated such that the two reagents are not concentrated together.

6.3.5 Summary of Results from Chemistry Studies

Looking deeper into the chemistry of the nickel-hydrazine system revealed that it is very sensitive to concentration and pH. When concentrated or in acidic media, the nickel-hydrazine complex was shown to polymerize into an insoluble metal-organic salt (Table 3 and Figure 20b). In low concentrations the complex does not polymerize and is relatively stable as a purple solution (Figure 20a). In basic media, the complex likely incorporates hydroxide to form an even more stable complex, identifiable as a royal blue solution.

The results explain why most early inks failed and why high temperature polyol-solvated inks only worked when the nickel concentration was low (0.05-0.10 M).

Implications of the study were that inks must be synthesized in a consistent order because the final state of the nickel (II) ion is sensitive to the order of addition of reagents.

Moreover, the previous assumption, that because hydrazine is sufficiently basic to provide thermodynamic favorability no additional base is necessary, was proven to be false. Moving forward, it was concluded that future formulations needed to include a strong base additive.

6.4 Low Temperature Inks in Strongly Basic Media

Since OH^- is a consumed reagent in the reduction reaction, its concentration has potential to affect the kinetics of the reaction and so the relatively low basicity provided by hydrazine could inhibit reduction speed. Furthermore, as demonstrated in the previous section, the lilac precipitant is soluble in strongly basic conditions making high $[\text{OH}^-]$ critical to ink solubility and thereby deposition performance.

It was thus hypothesized that providing basic conditions of pH greater than 13 via a strong base would enhance the thermodynamics and kinetics of the reduction while stabilizing the ink solution to ultimately facilitate metallization.

6.4.1 Proof of Concept: Sealed Vial Tests

A set of sealed vial tests was carried out to further validate that inclusion of a base would facilitate rapid metallization. The formulation studied was 0.1 M $[\text{Ni}^{2+}]$, 3.0 M $[\text{N}_2\text{H}_4]$, and 0.4 M $[\text{NaOH}]$ in 50 vol % of primary solvent and 50 vol % of H_2O . 0.1 M $[\text{Ni}^{2+}]$ was chosen to ensure a visually-significant amount of product. 30 mol N_2H_4 per mol Ni^{2+} is a common molar ratio in inks explored thus far. 0.4 M $[\text{NaOH}]$ corresponds to

the stoichiometric molar ratio in the reduction reaction and an initial pH of 13.6. The 50 vol % of water acted as a carrier for hydrazine and sodium hydroxide. Four primary solvents were chosen: water, ammonia solution, propylene glycol, and glycerol. Together the set covers a wide range of vapor pressures and functionalities.

10 mL of each formulation was combined into a sealable glass vial. First the alkaline water was added, followed by the primary solvent. The mixture was swirled, and then nickel acetate was added and mixed until the solution fully dissolved. The glass vial was capped to seal the system and then placed into a 48.5 °C water bath heated with a hot plate and mixed with a magnetic stirrer. The mixture was allowed 15 minutes to equilibrate with the water bath, and then hydrazine solution was added to complete the solution and initiate the reaction. Figure 21 shows the results of the sealed vial tests 30 minutes after addition of the hydrazine.

The results showed that reduction occurred in all media, but the result varies significantly solvent to solvent. For instance, material gathered at the bottom in water, but coated the walls and dispersed throughout the mixture in ammonia solution. In propylene glycol, the walls were again coated but the rest of the nickel agglomerated at the top.

From qualitative observation of color change, conclusions could be drawn on kinetics, which showed to be a key point of variation between solvents. Notably, the reaction was finished in ammonia solution and propylene glycol within minutes, whereas in water it took the majority of the 30-minute window. Glycerol in particular hindered the kinetics of the reaction so that by the 30-minute point only a portion of the reaction was finished, indicated by the strong blue hue still present in the solution phase.

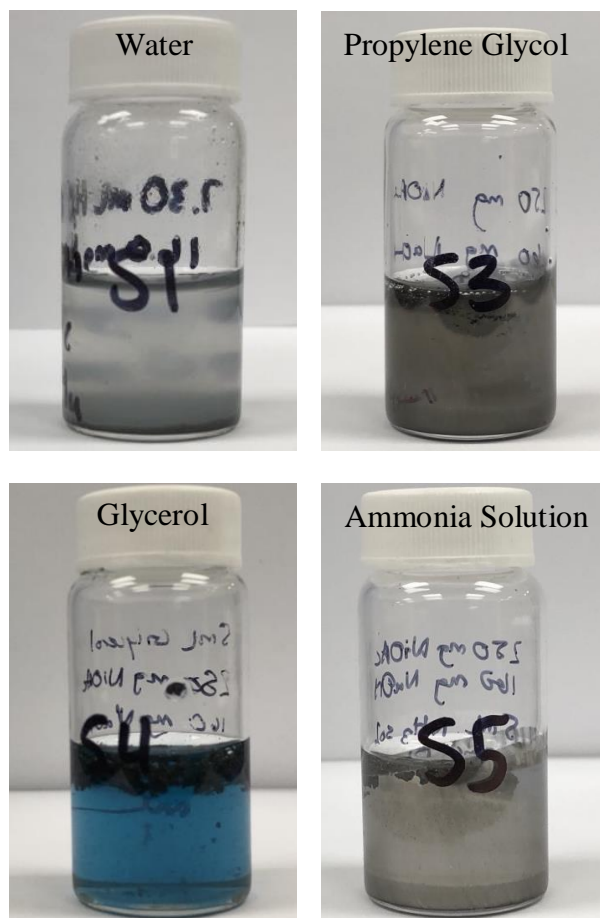


Figure 21. Sealed vessels containing 0.1 M $[\text{Ni}^{2+}]$, 3.0 M $[\text{N}_2\text{H}_4]$, and 0.4 M $[\text{NaOH}]$ in 50 vol % of primary solvent (listed on images) and 50 vol % of H_2O . Images are shown after 30 minutes of reaction at 48.5 °C.

6.4.2 pH-Enhanced Ammonia Inks

Two pH-enhanced ammonia-based formulations were studied varying the concentration of nickel acetate between 0.10 and 0.20 M $[\text{Ni}^{2+}]$. Otherwise, the composition was 1.8 M $[\text{N}_2\text{H}_4]$ and 0.4 M $[\text{NaOH}]$ in 16.7 vol % water and 83.3 vol % ammonia solution. These formulations are nearly identical to those in the previous NH_3 ink work (Section 6.2.1) except for the addition of 0.4 M $[\text{NaOH}]$ and higher $[\text{Ni}^{2+}]$.

Figure 22 provides optical microscopy of the samples.

As with the previous ammonia inks, the low viscosity again caused issues with forming a consistent droplet. However, the deposit does not show any colors, suggesting that it didn't reprecipitate nickel salt. Since metallization takes place rapidly relative to droplet evaporation, sodium reprecipitates onto the already formed nickel deposit, explaining why sodium salts constitute the majority of the deposit in the images (Figure 22).

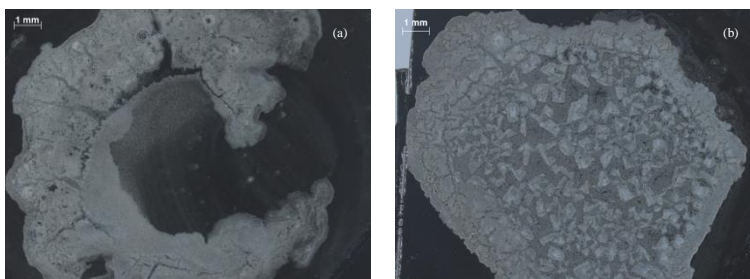


Figure 22. Optical images of pH-Enhanced NH_3 ink pipetted onto gold-coated silicon at $60\text{ }^\circ\text{C}$ containing $1.8\text{ M }[\text{N}_2\text{H}_4]$ $0.4\text{ M }[\text{NaOH}]$ and (a) $0.10\text{ M }[\text{Ni}^{2+}]$, (b) $0.20\text{ M }[\text{Ni}^{2+}]$ in $16.7\text{ vol } \% \text{ water}$ and $83.3\text{ vol } \% \text{ NH}_3 \text{ sol}$.

The EDS results (Table 5) showed significant contamination in the deposit. Sodium and hydroxide were explained by reprecipitation of the salt, but the source of carbon was less clear. Precipitation of the sodium-glycol compound observed in Chapter 6 explains a portion, but not the full $36.91\text{ atomic } \%$. Other possible sources include unreduced nickel acetate and polymerized glycol. Looking beyond contamination, the lack of nitrogen content in the first ink deposit indicated that the ink reduced instead of polymerizing. Increasing nickel acetate from 0.1 to 0.2 M while maintaining 0.4 M sodium hydroxide resulted in $4.65\text{ wt } \% \text{ nitrogen}$, suggesting nickel-hydrazine polymerization.

Table 5. EDS analysis of pH-Enhanced NH₃ ink deposits depicted in Figure 22 containing 1.8 M [N₂H₄] 0.4 M [NaOH] and (a) 0.10 M [Ni²⁺], (b) 0.20 M [Ni²⁺] in 16.7 vol % water and 83.3 vol % NH₃ sol.

<i>Element</i>	<i>0.10 M [Ni²⁺]</i>		<i>0.20 M [Ni²⁺]</i>	
	<i>Weight %</i>	<i>Atomic %</i>	<i>Weight %</i>	<i>Atomic %</i>
<i>Ni</i>	23	8	36	14
<i>Na</i>	28	24	27	27
<i>O</i>	26	31	21	29
<i>C</i>	23	37	12	23
<i>N</i>	0	0	5	8

Revisiting NH₃-based inks confirmed that addition of a strong base facilitated reduction where previously the nickel either reprecipitated as a salt or polymerized with hydrazine. The failed attempt to increase nickel precursor concentration suggested that excess strong base is likely necessary to maintain a high pH throughout the deposition.

Ultimately the results were promising and supported the design of future inks. However, use of ammonia as a primary solvent was again ineffective because of low viscosity and high vapor pressure; consequently, it was decided to discontinue use of ammonia solution as the bulk solvent in future work.

6.4.3 pH- and Solubility-Enhanced Propylene Glycol Inks

Propylene glycol inks were revisited because these act as a low-to-moderate temperature substitute for the glycerol inks, which were the most successful inks thus far. Furthermore, the vapor pressure of propylene glycol is well above hydrazine and other potential components. Thus, it is the last solvent to evaporate, and helps prevent the concentration of nickel in hydrazine solution. In this iteration, two limitations were addressed. Firstly, ammonia solution was added to the formulation to increase the

solubility of nickel acetate, thereby preventing particulation and stabilizing the solution. Secondly, a small amount of sodium hydroxide was added to the formulation also stabilizing the solution and additionally supporting the reduction reaction.

Three inks were generated according to the following formulations:

- 0.2 M $[\text{Ni}^{2+}]$, 3.0 M $[\text{N}_2\text{H}_4]$ and 0.1 M $[\text{NaOH}]$ in 1:5 ratio of NH_3 sol. to PG.
- 0.2 M $[\text{Ni}^{2+}]$, 3.0 M $[\text{N}_2\text{H}_4]$ and 0.4 M $[\text{NaOH}]$ in 1:5 ratio of NH_3 sol. to PG.
- 0.4 M $[\text{Ni}^{2+}]$, 3.0 M $[\text{N}_2\text{H}_4]$ and 0.4 M $[\text{NaOH}]$ in 1:5 ratio of NH_3 sol. to PG.

The constant volume of ammonia was chosen to ensure excess nickel solubility. The first two inks demonstrate low and high amounts of NaOH (pH 13.0 and 13.6, respectively). The third ink looks at an increased nickel concentration, enabled by ammonia addition.

The inks were pipetted at 75 °C. Results are shown in Figure 23. The first ink (Figure 23a) showed the familiar white material. As basicity increased (Figure 23b) the deposit showed less of the white material. The third ink which increased nickel concentration (Figure 23c) also contained white material, but it was visually different than previously.

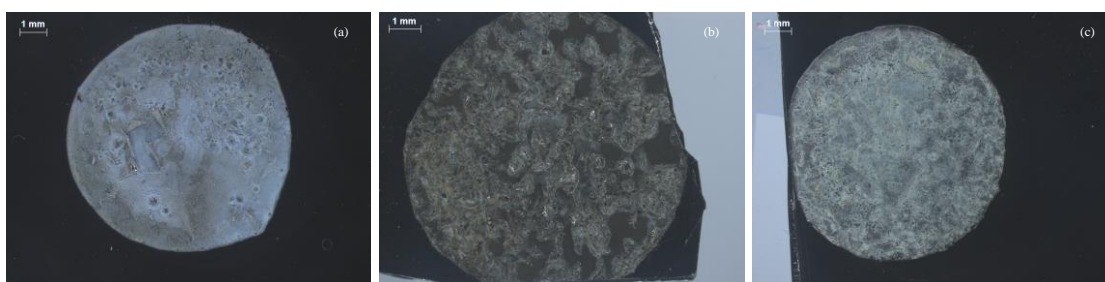


Figure 23. Optical images of PG-based inks pipetted onto gold-coated silicon at 75 °C. (a) 0.2 M $[\text{Ni}^{2+}]$, 0.1 M $[\text{NaOH}]$; (b) 0.2 M $[\text{Ni}^{2+}]$; 0.4 M $[\text{NaOH}]$; (c) 0.4 M $[\text{Ni}^{2+}]$, 0.4 M $[\text{NaOH}]$.

SEM of the first ink deposit (Figure 24) was difficult to capture due to charging effects, indicating an insulating material. Salt crystals are visible as the rigid shapes. The charging regions correspond to organics. Little to no signs of metal are visible. EDS analysis (Table 6) confirms the presence of polymer per the considerable nitrogen presence. The disparity in atomic % between sodium oxygen indicates that oxygen is retained in the deposit in more sources than just reprecipitated sodium hydroxide. Ultimately, results indicated that at 0.1 M [NaOH], there was insufficient hydroxide to drive reduction; consequently, the nickel favored polymerization.

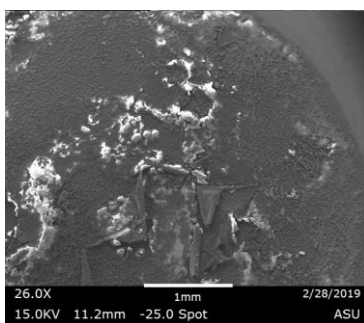


Figure 24. SEM of first pH-enhanced PG-based ink (0.2 M [Ni²⁺], 3.0 M [N₂H₄], and 0.1 M [NaOH] in 16.7 vol % water and 83.3 vol % PG) pipetted onto gold-coated silicon at 75 °C.

Table 6. EDS-sourced distribution of elements in deposit produced by second pH-enhanced PG ink deposit shown in Figure 24.

<i>Element</i>	<i>Weight %</i>	<i>Atomic %</i>
<i>Ni</i>	44	16
<i>Na</i>	9	9
<i>O</i>	18	25
<i>C</i>	17	32
<i>N</i>	11	18

SEM of the second ink deposit (Figure 25) showed significantly less charging than in the previous sample. The complex topology was associated with organic residue and precipitated sodium salts. EDS (Table 7) confirmed the organic residue per the carbon content. The greatly reduced nitrogen content supported that increased $[\text{OH}^-]$ facilitates reduction.

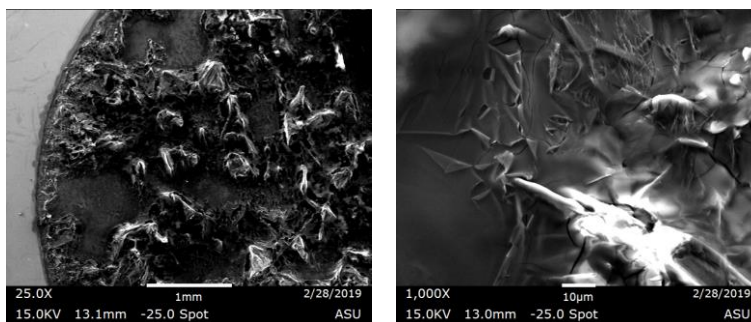


Figure 25. SEM of second pH-enhanced PG-based ink (0.2 M $[\text{Ni}^{2+}]$, 3.0 M $[\text{N}_2\text{H}_4]$, and 0.4 M $[\text{NaOH}]$ in 16.7 vol % water and 83.3 vol % PG) pipetted onto gold-coated silicon at 75 °C.

Table 7. EDS-sourced distribution of elements in deposit produced by second pH-enhanced PG ink deposit shown in Figure 25.

<i>Element</i>	<i>Weight %</i>	<i>Atomic %</i>
<i>Ni</i>	13	4
<i>Na</i>	25	19
<i>O</i>	30	32
<i>C</i>	29	42
<i>N</i>	2	3

SEM of the third ink deposit (Figure 26) showed a platelet structure associated with organic residue coating the surface. There also appeared to be nanoparticles dispersed across the surface, particularly visible at the boundary where the platelets end indicating that there might be a layer of nickel nanoparticles underneath the residue. EDS (Table 8)

confirmed the presence of organics. Carbon made up a smaller fraction previously.

Nitrogen remained small despite the doubling of initial nickel concentration.

The 2:1 ratio of oxygen to sodium indicated that oxygen was retained in the deposit in more than just reprecipitated sodium hydroxide, which was previously observed throughout this chapter. The other two possible sources in the known reaction space are nickel oxide and unreduced nickel acetate. XRD would aid in confirming the former. The lack of visible color or nitrogen content in the sample makes the latter unlikely. If the oxide is forming, it would be worthwhile to investigate carrying out deposition in an inert atmosphere like argon or nitrogen.

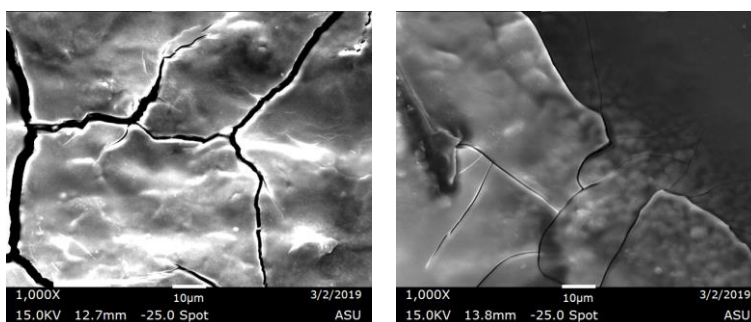


Figure 26. SEM of third pH-enhanced PG-based ink (0.4 M $[\text{Ni}^{2+}]$, 3.0 M $[\text{N}_2\text{H}_4]$, and 0.4 M $[\text{NaOH}]$ in 16.7 vol % water and 83.3 vol % PG) pipetted onto gold-coated silicon at 75 °C.

Table 8. EDS-sourced distribution of elements in deposit produced by third pH-enhanced PG ink deposit shown in Figure 26.

<i>Element</i>	<i>Weight %</i>	<i>Atomic %</i>
<i>Ni</i>	44	18
<i>Na</i>	15	15
<i>O</i>	23	33
<i>C</i>	16	31
<i>N</i>	2	3

6.4.4 Summary of pH-Enhanced PG Ink Study

Addition of NaOH successfully enhanced reaction rates. In samples with 0.4 M NaOH, metallization was consistently observed. Usually, the metal layer could be seen to form within moments of pipetting at temperatures 75 °C. In samples without sufficient NaOH concentration, the polymer was instead seen to rapidly form. Collectively, these results support the theory that basicity is playing a critical role in dictating whether the nickel reduces or polymerizes.

6.5 Byproducts Study

Carbon proved to be an unexpected but common contaminant in all inks presented within this chapter. To identify potential causes of carbon retention, a byproducts study was carried out. The study was conducted by mixing combinations of additives together onto glass slides heated to 75 °C (representative of ink deposition conditions). The mixtures were allowed to evaporate, and then the slides were studied with optical microscopy to identify any residue formations. Additionally, each individual samples of each additive were evaporated to act as controls.

As expected, all controls evaporated without leaving behind any discernable residue except for the sodium hydroxide which reprecipitated. All combinations of organics (N_2H_4 , NH_3 , and PG) also evaporated without producing a discernable residue.

A possible residue was first observed when sodium hydroxide was evaporated in PG. The PG evaporated much more slowly compared to its control. After drying what seemed to be two phases of material formed (Figure X). By contrast, the sodium hydroxide

reprecipitated normally when evaporated in N_2H_4 solution and NH_3 solution. Figure 27 shows images of sodium hydroxide precipitated in each solvent at 80 °C.

The residues produced from drying sodium hydroxide in DI water, ammonia solution, and hydrazine solution are relatively consistent. The coffee-stain effect is noticeable in how the bulk of precipitated sodium is in the boundary region of the droplets. The residue produced from drying in propylene glycol is noticeably different. There is a white inner-region of what appears to be precipitated sodium hydroxide surrounded by a clear, gelatinous substance that could be a polymer, sodium-glycol compound, or unevaporated propylene glycol resultant from boiling point elevation.

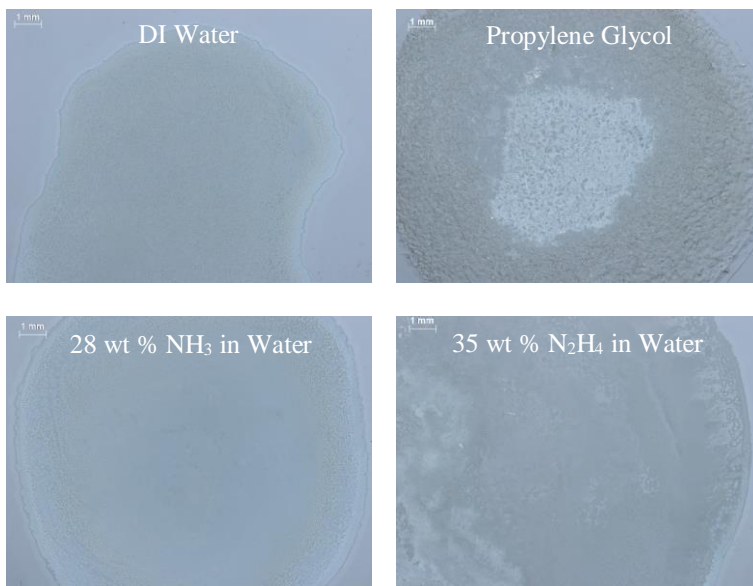


Figure 27. Residues produced by drying sodium hydroxide in various solvents (listed on images) for 1 hour at 80 °C.

The propylene glycol sample was reproduced on silicon and then coated in gold to facilitate further analysis with SEM and EDS.

The SEM (Figure 28) was very similar to many ink deposit samples which highlighted the detrimental effects of sodium contamination. Significant charging is visible, further confirming the presence of salt and organic matter.

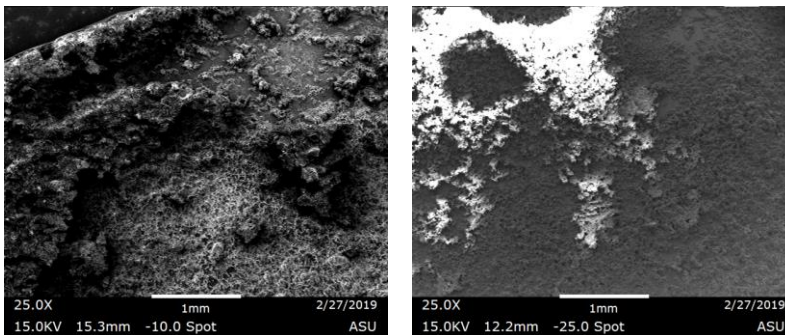


Figure 28. SEM of residue produced by drying NaOH in propylene glycol for 1 hour at 80 °C.

EDS (Table 9) detected a non-negligible carbon content, which confirmed carbon from propylene glycol was not entirely leaving via evaporation. The most likely explanation is a substitution reaction in which sodium replaces hydrogen in the alcohol groups on the glycol, resulting in a thermally-stable compound.

Table 9. EDS-Sourced Elemental Distribution in Byproduct Produced by Evaporating Propylene Glycol with Dissolved Sodium Hydroxide.

<i>Element</i>	<i>Weight %</i>	<i>Atomic %</i>
<i>Na</i>	43	33
<i>O</i>	46	51
<i>C</i>	11	16

6.6 Summary

The pH-Enhanced inks reported in this chapter demonstrated the potency of hydrazine as a reductant for nickel inks in sufficiently basic media. In all trials, the deposition visually finished within 5 to 30 seconds; much faster than previously. Furthermore, nitrogen content in the product was dramatically reduced or even eliminated, indicating that reduction was favored over polymerization.

Using sodium hydroxide to provide alkalinity contaminated the product with a thick layer of sodium compounds including sodium hydroxide itself, as well as what was suspected to be a sodium-glycol complex. Consequently, sodium hydroxide is not a viable hydroxide precursor for an optimal reactive ink. Moving forward, a volatile or decomposable alternative to sodium hydroxide that is inert with respect to propylene glycol is required so that the inks yield a high-purity metal, with no inorganic contamination and minimal organic contamination.

CHAPTER 7

LOW TEMPERATURE INKS USING TMAH

7.1 Introduction

Chapter 6 reported some low to moderate temperature inks using sodium hydroxide to supply hydroxide ions for the reduction reaction and maintain a strongly basic pH. EDS results indicated that that approach facilitated reduction of the nickel ions instead of polymerization. However, reprecipitated sodium contaminated the product limiting nickel content to 44% by mass in the best-case scenario.

Chapter 9 investigates tetramethylammonium hydroxide (TMAH) as alternative to sodium hydroxide. TMAH is similarly a strong base, but it begins to decompose into various simple organic compounds at about 100 °C. Moreover, the TMA cation is relatively inert per steric hindrance of the ammonia by methyl groups.

The inks studied here use the pH and solubility-enhanced PG inks reported in chapter 6 as a base design. In accordance, a nickel precursor (nickel acetate) is combined with a reductant (hydrazine) and base (TMAH here or NaOH previously) in a primary solvent with high solubility (e.g. ammonia solution) and a secondary solvent (propylene glycol). Three primary solvents were deemed worth studying including DI water, ammonia solution, and ethylamine. DI water is the most environmentally friendly and least reactive but provides the least solubility. Ammonia solution offers the best solubility and is chemically similar to the base. Ethylamine solution also provides considerable solubility and is an order of magnitude more basic than ammonia solution, thus maintaining a more basic solution pH as the primary base, TMAH, is consumed.

The work begins with a proof of concept study utilizing XRD to confirm that in a sealed vial scenario, an ink containing TMAH can produce metallic nickel. Then, some pipette tests are reported to show the performance of TMAH as a substitute for NaOH. Lastly, elect inks are dispense printed onto silicon for analysis with SEM, EDS, and XRD to characterize performance.

7.2 Proof of Concept: Sealed Vial Tests Employing TMAH

Samples for XRD were synthesized according to a base composition of 0.05 M $[\text{Ni}^{2+}]$, 2.2 M $[\text{N}_2\text{H}_4]$, and 0.28 M $[\text{TMAH}]$ in 30/30/40 vol % of DI water, primary solvent, and propylene glycol, respectively. The 30 vol % of DI water comes from its use as a carrier for hydrazine and TMAH. Three primary solvents were tested: DI water, ammonia solution, and ethylamine. Figure X provides individual XRD results for each formulation. Figure X overlays the results for easier comparison.

In all cases, the synthesis was carried out in a sealed glass vial, submerged in a well-mixed and water bath maintained at 60 °C. After 20 minutes of reaction, vials were removed from the water. Contents were transferred to centrifuge tube and then centrifuged for 5 minutes. The supernatant was pipetted off, and then the samples were rinsed with DI water. This process was repeated three times, and then the samples were dried at 120 °C in an oven.

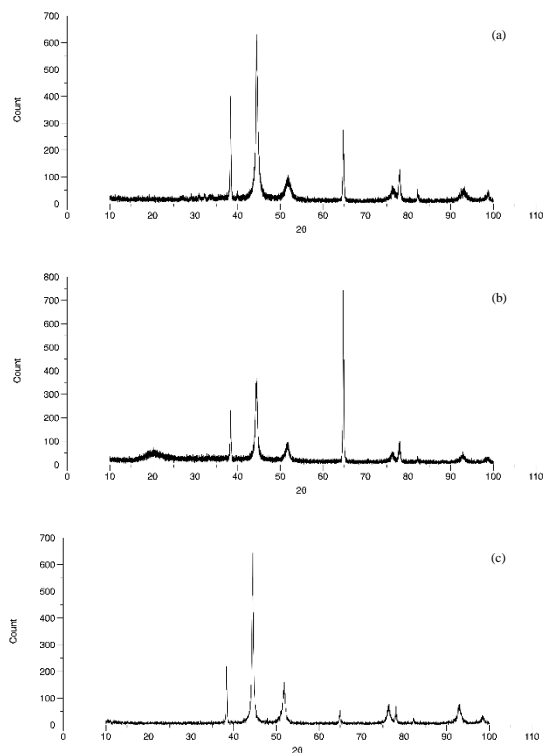


Figure 29. XRD scans of samples synthesized in sealed vials at 60 °C using the formulation 0.05 M $[\text{Ni}^{2+}]$, 2.2 M $[\text{N}_2\text{H}_4]$, and 0.28 M $[\text{TMAH}]$ in 30/30/40 vol % mix of DI water, primary solvent, and propylene glycol. The primary solvent is (a) ammonia solution; (b) ethylamine; (c) water.

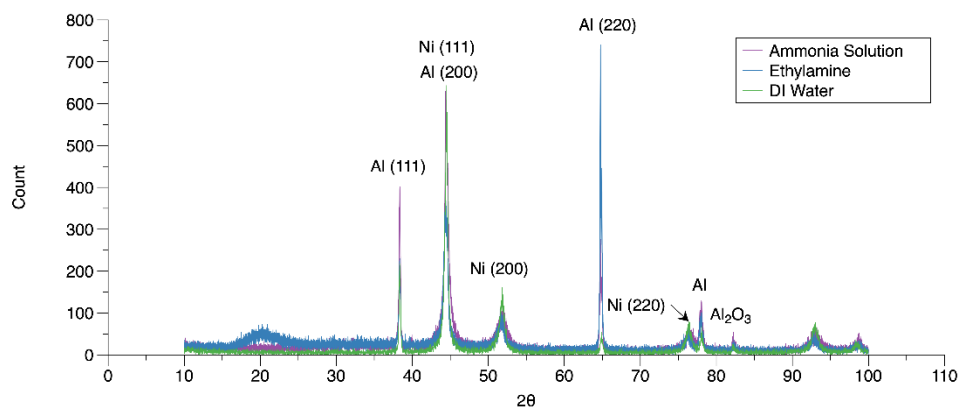


Figure 30. Overlaid XRD of samples synthesized in sealed vial tests at 60 °C using the formulation 0.05 M $[\text{Ni}^{2+}]$, 2.2 M $[\text{N}_2\text{H}_4]$, and 0.28 M $[\text{TMAH}]$ in 30/30/40 vol % of DI water, primary solvent, and propylene glycol, respectively. See legend for primary solvent.

Key nickel diffraction peaks including (111), (200), and (220) are present at 44°, 52°, and 76°. The other significant peaks at 38°, 65°, 78°, and 98° are attributed to the aluminum slide used as a sample mount. The study confirmed that the TMAH is capable of replacing NaOH as the base, and that the resultant ink can produce nickel.

7.3 Pipetting Enhanced PG Inks Using TMAH as a Base

The next step was to test TMAH in non-ideal conditions via pipette tests. Initially, three formulations were tested, each corresponding an ink used in proof of concept tests:

- 0.05 M [Ni²⁺], 1.84 M [N₂H₄], 0.4 M [TMAH] in a 30/70 vol % mix of NH₃ sol./PG
- 0.05 M [Ni²⁺], 1.84 M [N₂H₄], 0.4 M [TMAH] in a 30/70 vol % mix of EA/PG
- 0.05 M [Ni²⁺], 1.84 M [N₂H₄], 0.4 M [TMAH] in a 30/70 vol % mix of water/PG

Inks were produced by mixing the primary and secondary solvents together (i.e. NH₃ solution and PG for ink 1), adding nickel acetate, and then swirling the mixture until the salt dissolved. After dissolution, TMAH solution was pipetted in and the mixture was swirled until the color stabilized. Lastly, hydrazine solution was pipetted.

Pipetting the inks onto gold-coated glass slides at both 75 °C and 100 °C yielded promising results. There was not significant variation with respect to temperature. Almost immediately after droplets settled on the substrate, the color darkened as the gold nanoparticles catalyzed growth of an initial thin film. Shortly thereafter metal could be seen reducing out of the solution and forming the flakes seen in the microscopy (Figures X and X). Once solvents evaporated, only patchy metallic flakes remained. No visible residues were observed. The patchiness was attributed to the poor adhesion of the gold nanoparticles. The underside of the samples (not shown) appeared smooth and metallic.

The reflective metallic flakes produced in the pipette tests visually contrasted with the black aggregates of nanoparticles produced in sealed vial tests. This phenomenon is attributed to the gold catalytic coating, which facilitates film growth versus randomly-nucleated particle growth.

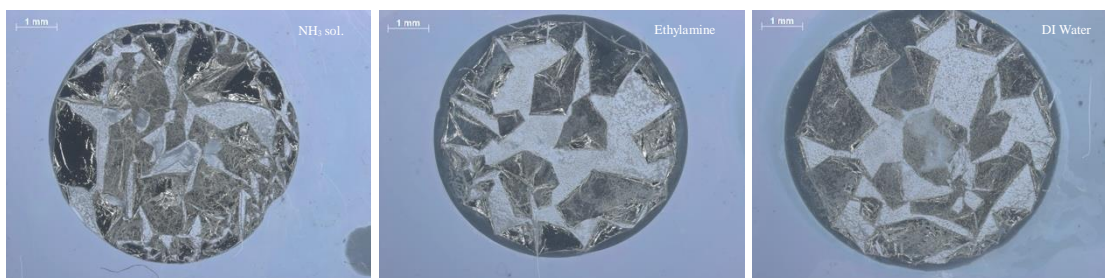


Figure 31. Deposits produced by pipetting inks (0.05 M $[\text{Ni}^{2+}]$, 1.84 M $[\text{N}_2\text{H}_4]$ and 0.4 M $[\text{TMAH}]$ in a 20/30/50 vol % mix of DI water, primary solvent, and PG respectively) onto a gold-coated glass slide at 75 °C. The primary solvent is labeled in the image.



Figure 32. Deposits produced by pipetting inks (0.05 M $[\text{Ni}^{2+}]$, 1.84 M $[\text{N}_2\text{H}_4]$ and 0.4 M $[\text{TMAH}]$ in a 20/30/50 vol % mix of DI water, primary solvent, and PG respectively) onto a gold-coated glass slide at 100 °C. The primary solvent is labeled in the image.

7.4 Printing Enhanced PG Inks using TMAH as a Base

Preliminary pipette tests on gold-coated glass slides were successful. From optical microscopy, inks produced broken up patches of nickel without a significant visual residue. The next step was to test printing. In this section, the three PG-enhanced inks (containing ammonia solution, ethylamine, and water) were printed separately onto glass and silicon for SEM, EDS, and XRD analysis to quantify the performance of the inks.

7.4.1 DI Water

Optical microscopy of printed samples for the DI water-solvated ink is shown for depositions at 75 °C (Figure 33) and 100 °C (Figure 34) on both glass and silicon. On glass the samples looked highly metallic although a clear residue was visible coating the sample and a large radius around it. The nickel metallized as distinct flakes rather than a uniform film. On silicon the nickel formed as a thin and uniform film. The material looked to be the same between temperatures but the deposits varied in shape. This was attributed to wetting, which decreased with respect to increasing temperature.

SEM and EDS were carried out on the 100 °C sample deposited on silicon. SEM (Figure 35) was difficult to capture due to charging. The silicon substrate was visible and it was difficult to find distinct examples of metal. Organics were dispersed across the sample. EDS (Table 10) measured only 25.74 wt % nickel. For reference, high temperature glycerol-based inks usually contained around 70 wt % nickel. There was a significant carbon presence (33.23 % by weight and 65.76 % by atomic), attributed to the residue observed in microscopy. No nitrogen was detected suggesting pH and temperature conditions were sufficient to promote reduction.

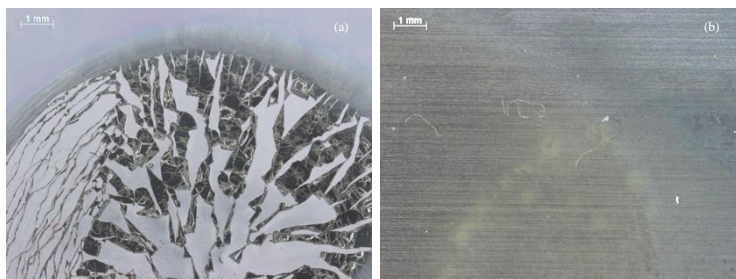


Figure 33. Images of deposits produced by printing ink (0.05 M $[\text{Ni}^{2+}]$, 1.84 M $[\text{N}_2\text{H}_4]$ and 0.4 M $[\text{TMAH}]$ in a 50/50 vol % mix of DI water and PG) at 75 °C onto gold-coated (a) glass; (b) silicon.

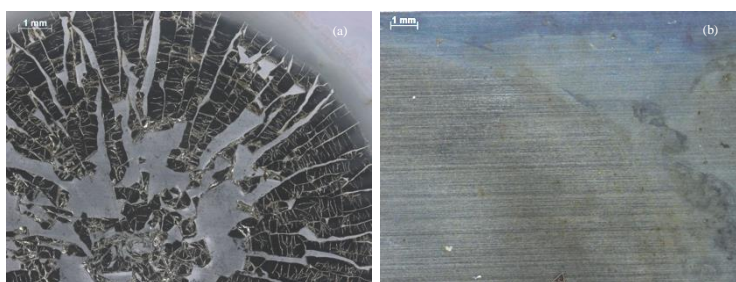


Figure 34. Images of deposits produced by printing ink (0.05 M $[\text{Ni}^{2+}]$, 1.84 M $[\text{N}_2\text{H}_4]$ and 0.4 M $[\text{TMAH}]$ in a 50/50 vol % mix of DI water and PG) at 100 °C onto gold-coated (a) glass; (b) silicon.

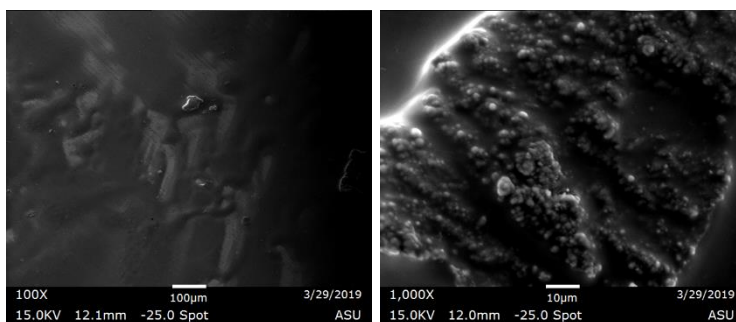


Figure 35. SEM of deposit produced by printing ink (0.05 M $[\text{Ni}^{2+}]$, 1.84 M $[\text{N}_2\text{H}_4]$ and 0.4 M $[\text{TMAH}]$ in a 50/50 vol % mix of DI water and PG) at 100 °C onto gold-coated silicon.

Table 10. Elemental weight and atomic distributions in deposit produced by printing ink (0.05 M [Ni²⁺], 1.84 M [N₂H₄] and 0.4 M [TMAH] in a 50/50 vol % mix of DI water and PG) at 100 °C onto gold-coated silicon.

<i>Element</i>	<i>Weight %</i>	<i>Atomic %</i>
<i>Ni</i>	26	7
<i>O</i>	26	27
<i>C</i>	48	66
<i>N</i>	-	-

7.4.2 Ammonia Solution

Optical microscopy of printed samples for the ammonia-solvated ink is shown for depositions at 75 °C (Figure 36) and 100 °C (Figure 37) on both glass and silicon. Optical images looked very similar to those the samples using DI water as the primary solvent. Temperature again only appeared to affect deposit shape. As with the DI water ink, the deposited product was dissimilar on glass compared to silicon. On glass, flakes formed, and the residue was thin. On silicon, a film formed, and the residue was thick. Two layers were printed onto the silicon samples versus one on glass. The thickness of residue can likely be attributed to the extra layer.

SEM and EDS were carried out on the 100 °C sample deposited on silicon. SEM (Figure 38) was again difficult to capture, and little was visible except for the silicon substrate with a black material sporadically deposited atop. EDS (Table 11) showed that the ammonia-based ink contained much higher nickel content compared to the water-based ink (54.12 wt % vs. 25.74 wt %) indicating that less carbon was retained in the deposit. The lack of nitrogen also indicated that no nickel-hydrazine polymer formed.

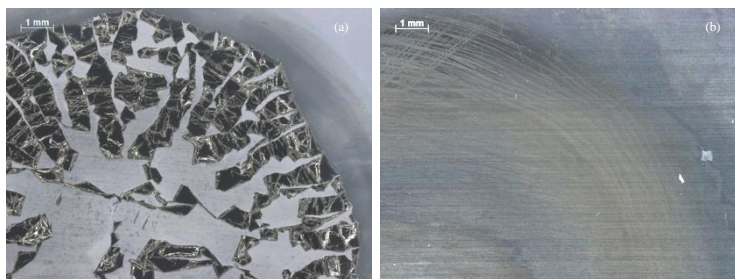


Figure 36. Images of deposits produced by printing ink (0.05 M $[\text{Ni}^{2+}]$, 1.84 M $[\text{N}_2\text{H}_4]$ and 0.4 M $[\text{TMAH}]$ in a 20/30/50 vol % mix of DI water, ammonia solution, and PG respectively) at 75 °C onto gold-coated (a) glass; (b) silicon.

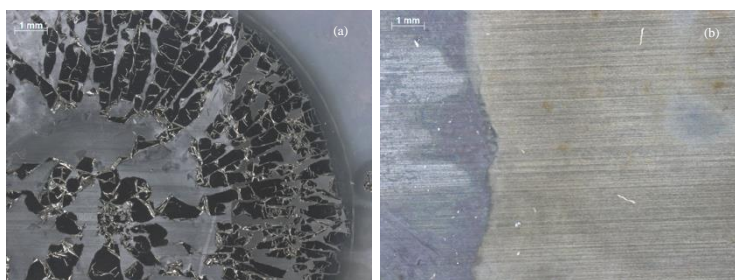


Figure 37. Images of deposits produced by printing ink (0.05 M $[\text{Ni}^{2+}]$, 1.84 M $[\text{N}_2\text{H}_4]$ and 0.4 M $[\text{TMAH}]$ in a 20/30/50 vol % mix of DI water, ammonia solution, and PG respectively) at 100 °C onto gold-coated (a) glass; (b) silicon.

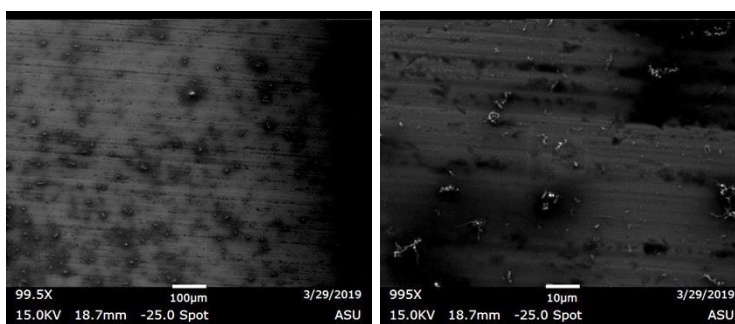


Figure 38. SEM of deposit produced by printing ink (0.05 M $[\text{Ni}^{2+}]$, 1.84 M $[\text{N}_2\text{H}_4]$ and 0.4 M $[\text{TMAH}]$ in a 20/30/50 vol % mix of DI water, ammonia solution, and PG respectively) at 100 °C onto gold-coated silicon.

Table 11. Elemental weight and atomic distributions in deposit produced by printing ink (0.05 M [Ni²⁺], 1.84 M [N₂H₄] and 0.4 M [TMAH] in a 20/30/50 vol % mix of DI water, ammonia solution, and PG respectively) at 100 °C onto gold-coated silicon.

<i>Element</i>	<i>Weight %</i>	<i>Atomic %</i>
<i>Ni</i>	54	21
<i>O</i>	13	18
<i>C</i>	33	62
<i>N</i>	-	-

7.4.3 Ethylamine Solution

Optical microscopy of printed samples for the ethylamine-solvated ink is shown for depositions at 75 °C (Figure 36) and 100 °C (Figure 37) on both glass and silicon. Little changed from using ethylamine as the primary solvent except for the formation of a new byproduct on silicon substrate, visible as dark specs in the microscopy (Figures 39b and 40b). Temperature had a more significant effect than previously on the uniformity of the glass-deposited samples. At 75 °C the metal was sparsely deposited with large gaps in between flakes. At 100 °C the spread across the surface more uniformly, resulting in only a small portion of the substrate showing through.

SEM and EDS were carried out on the 100 °C sample deposited on silicon. SEM (Figure 39) showed a rough surface coated in organics. The organics were thought to be the dark specs visible in microscopy. EDS showed nickel and carbon contents similar to the water ink. Some nitrogen (5.85 wt % by mass) was detected, suggesting some polymerization occurred. From SEM and EDS, the ethylamine ink seemed to perform the worst of the three tested in this chapter.

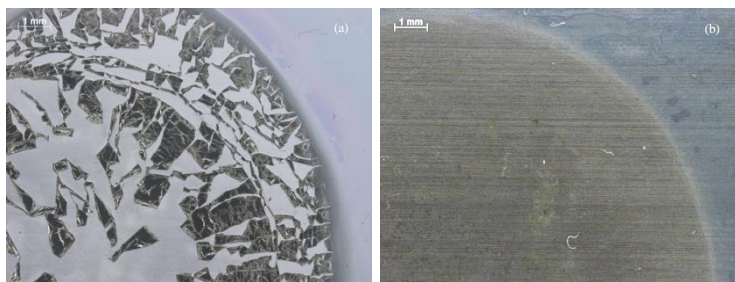


Figure 39. Deposits produced by printing ink (0.05 M $[\text{Ni}^{2+}]$, 1.84 M $[\text{N}_2\text{H}_4]$ and 0.4 M $[\text{TMAH}]$ in a 20/30/50 vol % mix of DI water, ethylamine solution, and PG respectively) at 75 °C onto gold-coated (a) glass; (b) silicon.

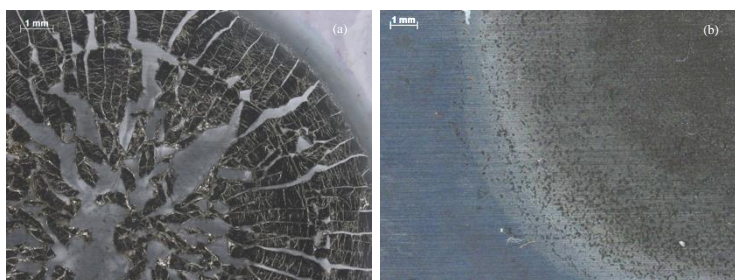


Figure 40. Deposits produced by printing ink (0.05 M $[\text{Ni}^{2+}]$, 1.84 M $[\text{N}_2\text{H}_4]$ and 0.4 M $[\text{TMAH}]$ in a 20/30/50 vol % mix of DI water, ethylamine solution, and PG respectively) at 100 °C onto gold-coated (a) glass; (b) silicon.

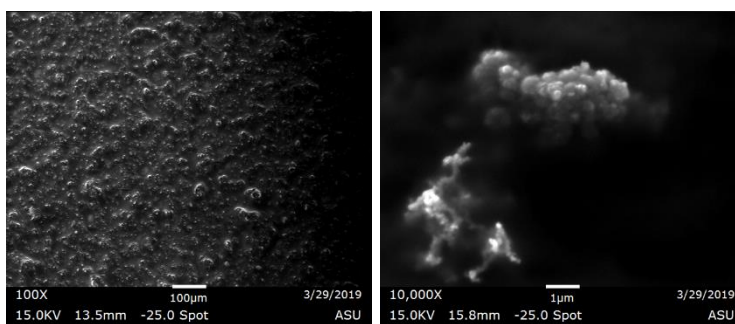


Figure 41. SEM of deposit produced by printing ink (0.05 M $[\text{Ni}^{2+}]$, 1.84 M $[\text{N}_2\text{H}_4]$ and 0.4 M $[\text{TMAH}]$ in a 20/30/50 vol % mix of DI water, ethylamine solution, and PG respectively) at 100 °C onto gold-coated silicon.

Table 12. Elemental weight and atomic distributions in deposit produced by printing ink (0.05 M [Ni²⁺], 1.84 M [N₂H₄] and 0.4 M [TMAH] in a 20/30/50 vol % mix of DI water, ethylamine solution, and PG, respectively) at 100 °C onto gold-coated silicon.

<i>Element</i>	<i>Weight %</i>	<i>Atomic %</i>
<i>Ni</i>	28	8
<i>O</i>	18	18
<i>C</i>	49	67
<i>N</i>	6	7

7.5 Analyzing Deposition on Glass

The marked difference between deposits printed on glass versus silicon raised questions of whether the substrate was affecting the nature of the product. To investigate, SEM and EDS were carried the ethylamine-solvated ink printed at 100 °C (Figure 37a). SEM is provided in Figure 42, elemental spot maps in Figure 43, and elemental distribution in Table 13.

SEM (Figure 42) showed large flakes of nickel deposited onto the substrate with sporadic clumps of residue spread across. From the spot maps (Figure 43), nickel was concentrated in the flakes but was also consistently detected in between, likely as nanoparticles. Carbon and oxygen were relatively uniform in spread suggesting that these elements are likely contained in the residue. There were also a few detections of nitrogen (2.41 wt %) suggesting some polymerization; consistent with EDS analysis on silicon.

EDS showed significant carbon content (26.23 wt %); more than previous inks but less than the same ink deposited on silicon. The increase in carbon relative to previous inks supported that TMAH was involved in residue formation. The decrease with respect

to deposition on silicon indicated that the second layer deposited onto silicon likely failed; a result that can be attributed to the residue inhibiting catalysis. The spot map for silicon outlined the spots where the glass substrate can be seen in the SEM. By contrast, the spot map for oxygen is relatively uniform across the deposit. This indicated that oxygen was being detected in either the metal or residue and not just the substrate (glass).

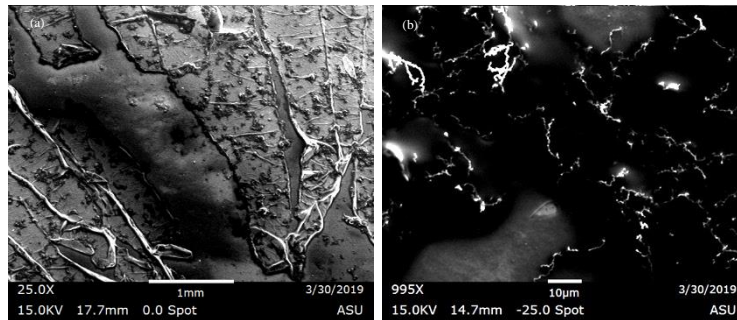


Figure 42. SEM of deposit produced by printing ink (0.05 M $[\text{Ni}^{2+}]$, 1.84 M $[\text{N}_2\text{H}_4]$ and 0.4 M $[\text{TMAH}]$ in a 20/30/50 vol % mix of DI water, ethylamine solution, and PG respectively) at 100 °C onto a gold-coated glass slide. Images show (a) nickel flakes; (b) residue on flakes.

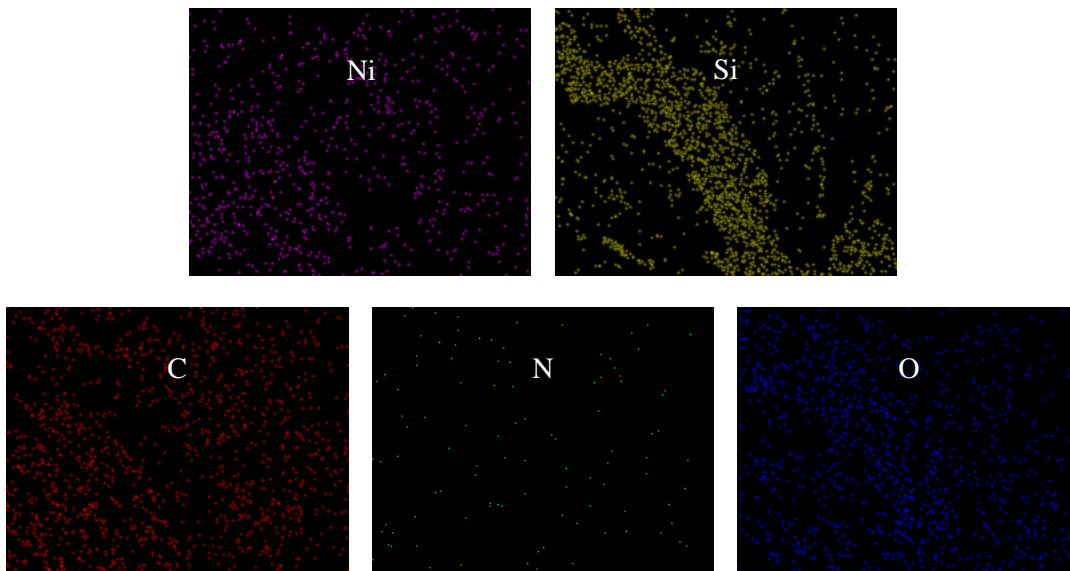


Figure 43. Elemental spot maps composed by EDS on deposit produced by printing ink (0.05 M $[\text{Ni}^{2+}]$, 1.84 M $[\text{N}_2\text{H}_4]$ and 0.4 M $[\text{TMAH}]$ in a 20/30/50 vol % mix of DI water, ethylamine solution, and PG respectively) at 100 °C onto a gold-coated glass slide. Deposit shown in Figure 37a.

Table 13. Elemental weight and atomic distributions in deposit produced by printing ink (0.05 M [Ni²⁺], 1.84 M [N₂H₄] and 0.4 M [TMAH] in a 20/30/50 vol % mix of DI water, ethylamine solution, and PG, respectively) at 100 °C onto gold-coated glass.

<i>Element</i>	<i>Weight %</i>	<i>Atomic %</i>
<i>Ni</i>	56	22
<i>O</i>	16	23
<i>C</i>	26	51
<i>N</i>	2	4

7.5.1 Discussion of Printing Results

Printed samples on glass were visually consistent with pipetted samples. Printed samples on silicon varied significantly; the metal appeared as a film versus a collection of flakes on glass. Since the spottiness observed in glass samples was attributed to poor adhesion of the catalytic gold layer, the differences could be due to the gold nanoparticles adhering better to silicon than glass. The crystallinity of the silicon wafers would also provide a more uniform base for film growth compared to amorphous glass and this likely contributed to the uniformity observed.

The other major difference between samples printed on silicon vs. glass was the presence of significantly more residue and byproduct. This was suspected to be a direct result of printing two layers. Firstly, the catalyst would change between layers; gold nanoparticles for the first, and deposited nickel for the second. Secondly, residue from the first layer interferes with deposition of the second.

The presence of residue was an unexpected result. There are three primary sources for carbon in ink reported here: acetate ions, tetramethylammonium (TMA) ions, and propylene glycol. Propylene glycol should evaporate during deposition. It is known to form polymers catalyzed by metals but unless the polymer reached significant molecular weights it would still be liquid at ambient conditions. TMAH and, by extension, TMA is expected to decompose into various volatile products at 100 °C. Similarly, the acetate ion is expected to bond with an H⁺ to form acetic acid, which is volatile at 100 °C. However, under the highly basic conditions caused by TMAH, the [H⁺] concentration approaches zero and formation of acetic acid would be unlikely. More likely is protonation of the acetate ion by the readily available TMA ion, forming tetramethylammonium acetate or some derivative of it.

Tetramethylammonium acetate is a white, coarse salt at ambient conditions with a melting point of 184 °C. If synthesized and crystallized slowly out of solution as droplets dried (~15-25 minutes), then it is possible that the material would form a thick, transparent residue on the deposit. One molecule of tetramethylammonium acetate would contain 14 carbon, 2 oxygen, and 1 nitrogen. In these inks, TMAH is present in 0.4 M and acetate in 0.1 M compared to 0.05 M concentration in these inks, compared to 0.05 M nickel. Thus, formation of such a byproduct could explain the residue.

Ultimately, this is only a hypothesis; NMR, XRD, and other standard techniques are necessary to confirm whether this side reaction is occurring. Nevertheless, introduction of TMAH as a base resulted in a drastic increase of carbon content in ink deposits. From these results, the inks presented in this chapter failed to meet design requirements and raised the question of whether TMAH is a viable source of hydroxide in future work.

7.6 Summary

Chapter 7 reported three ink archetypes: water-solvated, ammonia-solvated, and ethylamine-solvated. Other than the primary solvent, composition is consistent; nickel acetate acts as a nickel precursor, hydrazine as a reductant, TMAH as a base, and propylene glycol as a low vapor pressure additive.

Preliminary pipette tests on gold-coated glass deposited what appeared to be metallic flakes at temperatures ranging from 60 – 100 °C. Printing reproduced these deposits successfully after printing parameters were tuned. A transparent residue was visible on all samples; especially printed deposits which deposited greater volumes. An attempt to print several layers onto silicon for improved analysis failed, attributed to interference effects by the residue.

SEM and EDS revealed that organics, associated with the residue, made up as much as low as 50 % by weight and as high as 80 % of the deposits by weight. This was significantly greater than previous tests using NaOH as a base (Chapter 6), indicating that TMAH was likely playing a role. Upon reviewing possible sources, it was hypothesized that the residue was a product of side reactions between TMA and acetate ions; for instance, synthesis of tetramethylammonium acetate salt, which has a melting point of 184 °C and would therefore exist as a crystalline residue at ambient conditions.

Regardless of this hypothesis, the inks reported in this chapter failed to produce a sufficiently metallic (< 10 wt % organic) product, indicated that the reaction still needs modification to stop the formation of organic residues.

CHAPTER 8

CONCLUSIONS AND FUTURE WORK

8.1 Summary of Results

Hydrazine was investigated as a powerful reducing agent for formulating a particle-free and low temperature self-reducing nickel reactive ink. The bulk of literature on the reaction between nickel (II) and hydrazine are aimed at the synthesis of fine powders and nanoparticles. In these works, simple nickel (II) precursors (e.g. chloride, nitrate, and acetate salts) are combined with hydrazine and alkaline salts in aqueous media ($\text{pH} > 13$).

To test the applicability of this system to nickel reactive inks, a series of inks were synthesized containing 0.05 – 0.5 M $\text{Ni}(\text{CH}_3\text{CO}_2)_2$ and 0.25-5 M N_2H_4 . To avoid non-volatile compounds, ammonium hydroxide was included as a base in place of alkaline salts. Early on, inks were solvated in water. These inks were pipetted onto glass slides at temperatures ranging from ambient to 100 °C. In all iterations, the inks failed to metallize nickel. Instead, either nickel (II) salts reprecipitated or a material suspected to be a nickel-hydrazine polymer formed.

We initially thought that these results occurred because the droplets were evaporating before the reduction reaction had sufficient time to finish. To address this, three steps were taken. Firstly, DI water was replaced with glycerol to decrease bulk vapor pressure of droplets. Secondly, deposition temperatures were increased to the range 100 – 200 °C, enhancing reduction rates and better matching the volatility of glycerol. Thirdly, substrates were coated with gold-nanoparticles to catalyze reduction so that initiation occurs sooner.

These high temperature glycerol-based inks consistently produced metallic-looking product, although clear, thin residues were often be seen coating the metal. Further analysis with SEM and EDS confirmed 5-15 % carbon by weight and large oxygen content suggesting oxidation of the nickel. Carbon retention was attributed to a possible polymerization of glycerol, forming a solid organic residue. This would additionally account for a portion of the oxygen content. No nitrogen was detected, indicating that hydrazine evolved as gaseous byproducts instead of polymerizing with nickel.

Next, a series of low temperature inks were investigated. Initially the glycerol-based inks were reproduced at lower temperatures in higher vapor pressure solvents like ammonia, ethylene glycol, and propylene glycol. These failed, producing polymer instead of metal. Before attempting more tests, some chemistry studies were conducted to better understand conditions for reduction versus polymerization.

These studies revealed that the two reactions of nickel (II) and hydrazine are highly sensitive to pH. From literature, the thermodynamics of reduction are favorable at any pH but increase with respect to basicity. Regarding kinetics, there is no literature on reaction order with respect to $[\text{OH}^-]$ but from observation, the kinetics were greatly enhanced under at higher pH. Regarding polymerization, an insoluble lilac polymer formed immediately when nickel acetate and hydrazine solution were combined in acidic conditions. When the pH was increased by addition of NaOH, polymerization reversed; the precipitant rapidly dissolved to form a solution ranging from violet to royal blue according to agent concentrations. We concluded from these results that nickel inks were not reducing at low temperature because using ammonia solution, a weak base, the pH was insufficient to tune reaction selectivity towards reduction.

This theory was tested by repeating the previous low temperature inks with addition of sodium hydroxide. The effect on deposition was significant; rapid metallization was observed, followed by reprecipitation of the sodium on top as the droplet dried. Moreover, inks stayed solvated and did not change in color for at least a week, suggesting good stability. EDS did not detect nitrogen in most deposits produced by these inks, indicating that increasing the pH successfully drove the system to reduce instead of polymerize nickel (II) ions.

Adding sodium hydroxide to low temperature inks provided effective idea validation. However, alkaline salts are not viable additives in inks due to their non-volatility in temperature ranges studied here. TMAH was investigated as an organic alternative to sodium hydroxide in Chapter 7. Preliminary tests were promising as samples metallized rapidly upon exposure to heat and catalyst to form metallic flakes. A light residue was observed on some samples. Inks containing TMAH were dispense printed onto glass and silicon substrates for more intensive testing. In both cases, a thick coating of organic residue covered the deposits, making up as much as 80 % of deposits by weight according to EDS. Combined visual and EDS analysis suggested that nickel was metallized, but XRD results (Appendix B) were inconclusive in confirming metallization due to thinness of deposits. Residue inhibited catalytic activity of the surface thereby preventing deposition of multiple layers to facilitate better characterization.

Significantly more organic residue was observed in samples produced by inks containing TMAH, suggesting that it is a likely source. It was hypothesized that the TMA ion is bonding with acetate ions to form tetramethylammonium acetate, a crystalline salt at room temperature, although further work is necessary to conclude this.

Ultimately, particle-free nickel inks were reported that met the deposition temperature target of 100 °C or below but failed to meet purity targets due to the production of stable organic residues. Results showed hydrazine to be a potent reductant under proper conditions, but that the reaction space is expansive and includes competing reactions, side reactions and byproducts. Thus, this work provides a framework for further development.

8.2 Recommendations

Results in this study were promising up until the final chapter which indicated that the current ink composition is incompatible and produces non-volatile byproducts via side reactions. It is recommended to revisit the chemistry to fully develop our understanding of the reaction space including developing a comprehensive identification and characterization of byproducts and side reactions. The following recommendations discuss the strengths and limitations of the chosen ink components, then provide alternatives to consider for designing future iterations.

8.2.1 Nickel Precursor

Nickel acetate was chosen as the nickel (II) precursor because it is soluble in a variety of media including water, ammonia, alcohols, amines, and more. Moreover, the acetate anion tends to form acetic acid in solution, which is volatile at 100 °C. Chapter 7 showed that TMAH might be forming tetramethylammonium acetate, a non-volatile salt, with nickel acetate. To address this residue, it is worth considering alternative precursors for nickel. Common counterions include halides (i.e. Br, Cl, F, I), organic acids salts (e.g. acetate, formate, citrate), basic salts (e.g. oxyfluoride), hydroxide, and more.

Halides are soluble in common solvents but tend to evolve hazardous vapors (e.g. HCl) from deposition and are thus not ideal. Moreover, the TMA ion readily reacts with halides to form salts having melting points over 400 °C.

Organic acids are more ideal by comparison; these are also usually soluble in a wide range of media and tend to evolve less hazardous byproducts. Formate is a particularly interesting counterion because it is a moderately effective reductant itself. Furthermore, the tetramethylammonium formate salt is liquid at ambient conditions and boils at 100 °C; therefore, it would not produce a lasting residue in these inks.

Basic salts are an interesting case because they would contribute both nickel and base, making inclusion of a separate base additive redundant. However, these precursors are less common and consequently there is little literature available to understand critical parameters like solubility, volatility, reactivity, etc.

Hydroxide is a particularly interesting case because, like basic salts, Ni(OH)₂ would contribute both nickel and hydroxide to the ink. The salt was not considered for this work because it is soluble in acid and ammonia, but not water or most other media. Since hydrazine is only strong in basic media, acidic conditions are not suitable. However, hydroxide is also soluble in ammonia. If complications persist, it would be worth investigating a low temperature ink containing nickel hydroxide and hydrazine solvated in ammonia solution. This would reduce the number of components to offer clean route to metallization with a significantly constrained reaction space.

From these analyses, formate and hydroxide show the most promise as counterions to replace acetate. Formate would build off the inks presented in this work as it would behave similarly to acetate. Hydroxide would require a more revised approach.

8.2.2 Reducing Agent

Hydrazine was chosen because there is extensive literature on its use as a reductant for producing pure metallic nickel from the nickel (II) ion in basic aqueous media. Nearly all other common reductants produce a doped form of nickel (i.e. Ni-P or Ni-B). Overall, hydrazine was effective for this work, but its reactivity introduced some problems including formation of polymer and potential side reactions.

Hydrazine is well-known to be highly reactive and this work showcased the extent of its potency in how it was capable of polymerizing nickel. The ability to polymerize nickel comes from a combination of hydrazine's small size and strong reducing potential. Under standard conditions, hydrazine is more than capable of thermodynamically favorable reduction. In molar ratios of 5-30, as applied here, the reduction potential is in far excess. Therefore, there is adequate room to modify the hydrazine molecule with alkyl or other groups in order to reduce its potency and add steric hinderance. Together, these effects might inhibit the polymerization reaction so that reduction is favored even in pHs lower than 13, which would open up the choice of base additive to include weaker bases like ammonia or ethylamine.

Looking at alternatives to hydrazine, the formate ion is a suitable contender. In strongly basic media and high concentration, formate can be a potent reductant. Ginley et al.²⁷ used formate to develop one of the only reported nickel reactive inks. In their ink, formate was provided in high concentration via the nickel formate precursor. The ink reduced at around 200 °C, but this might be lowered by inclusion of a strong base, such as TMAH, to increase the reduction potency.

8.2.3 Solvent

In general, solvents should be chosen to provide good solubility for the precursor and agents, as well as provide a suitable vapor pressure to facilitate the desired reaction temperature. In this work, solvent selection may also take into account chemical effects; for instance, ammonia acts as an effective complexing agent to block formation of the nickel-hydrazine polymer. Generally, the solvent should complex with nickel (II) better than hydrazine in order to inhibit.

In the culminating inks of this work, two solvents were combined: a primary solvent (DI water, ammonia, or ethylamine) and a polyol (EG or PG). The primary solvent provided the solubility requirement while the secondary solvent provided other desirable effects like low-to-moderate vapor pressure and surfactant activity. This seems the optimal approach until the rest of the system is optimized to reduce easily and rapidly. Then, work should aim to replace the secondary polyol solvent with a water or a water-like solvent that is volatile at 70-100 °C and is, ideally, environmentally friendly.

8.2.4 Base Additive

As discussed, hydrazine requires strongly basic media to act as a reductant. Early in this work ethylamine and ammonia solution were employed as weak bases to provide pH ranging from 11-13. Under these conditions, the system usually polymerized instead of reducing.

Replacing weak bases with strong bases like NaOH led to metallization in Chapter 6. In retrospect, this is consistent with nanoparticle literature which includes strong bases concentrated upwards of 1.0 M to provide hydroxide in significant excess.

TMAH seemed an optimal replacement for NaOH but the residues observed indicated that it is likely incompatible with one or more other formulants. It was hypothesized that acetate was the primary incompatibility; this should be confirmed before making further decisions. Tetramethylammonium acetate (TMAA) is readily available for purchase with common sellers like SigmaAldrich. It is recommended to purchase a sample, analyze the crystals with powder XRD, and then compare the spectrum to the inks observed in XRD.

If the incompatibility lies with acetate, then one should be replaced. Alternatives to acetate are discussed in Section 8.2.1. Alternatives to TMAH are rarer, but there is literature on strongly basic organic molecules that have been synthesized for various applications.

REFERENCES

- (1) Singh, M.; Haverinen, H. M.; Dhagat, P.; Jabbour, G. E. Inkjet Printing-Process and Its Applications. *Adv. Mater.* **2010**, *22* (6), 673–685.
- (2) Calvert, P. Inkjet Printing for Materials and Devices. *Chem. Mater.* **2001**, *13* (10), 3299–3305.
- (3) Li, J.; Rossignol, F.; Macdonald, J. Inkjet Printing for Biosensor Fabrication: Combining Chemistry and Technology for Advanced Manufacturing. *Lab Chip* **2015**, *15* (12).
- (4) Boland, T.; Xu, T.; Damon, B.; Cui, X. Application of Inkjet Printing to Tissue Engineering. *Biotechnol. J.* **2006**, *1* (9), 910–917.
- (5) De Gans, B. J.; Duineveld, P. C.; Schubert, U. S. Inkjet Printing of Polymers: State of the Art and Future Developments. *Adv. Mater.* **2004**, *16* (3), 203–213.
- (6) Curtis, C.; Rivkin, T.; Miedaner, a; Alleman, J.; Perkins, J.; Smith, L.; Ginley, D. Metallizations by Direct-Write Inkjet Printing. *NCPV Progr. Rev. Meet. Direct-write Technol. Offer potential low-cost, Mater. Depos. contact Met. PV.* **2001**, No. October.
- (7) Cummins, G.; Desmulliez, M. P. Y. Inkjet Printing of Conductive Materials: A Review. *Circuit World* **2012**, *38* (4), 193–213.
- (8) Chen, S.-P.; Chiu, H.-L.; Wang, P.-H.; Liao, Y.-C. Inkjet Printed Conductive Tracks for Printed Electronics. *ECS J. Solid State Sci. Technol.* **2015**, *4* (4).
- (9) Walker, S. B.; Lewis, J. A. Reactive Silver Inks for Patterning High-Conductivity Features at Mild Temperatures. **2011**, No. I, 1–6.
- (10) Persaud, K. C. Polymers for Chemical Sensing. *Mater. Today* **2005**, *8* (4), 38–44.
- (11) Mortimer, R. J.; Dyer, A. L.; Reynolds, J. R. Electrochromic Organic and Polymeric Materials for Display Applications. *Displays* **2006**, *27* (1), 2–18.
- (12) Angelopoulos, M. Conducting Polymers in Microelectronics. *IBM J. Res. Dev.* **2010**, *45* (1), 57–75.
- (13) Wu, Y.; Li, Y.; Liu, P.; Gardner, S.; Ong, B. S. Studies of Gold Nanoparticles as Precursors to Printed Conductive Features for Thin-Film Transistors. *Chem. Mater.* **2006**, *18* (19), 4627–4632.

- (14) Cui, W.; Lu, W.; Zhang, Y.; Lin, G.; Wei, T.; Jiang, L. Gold Nanoparticle Ink Suitable for Electric-Conductive Pattern Fabrication Using in Ink-Jet Printing Technology. *Colloids Surfaces A Physicochem. Eng. Asp.* **2010**, 358 (1–3), 35–41.
- (15) Chang, C. W.; Cheng, T. Y.; Liao, Y. C. Encapsulated Silver Nanoparticles in Water/Oil Emulsion for Conductive Inks. *J. Taiwan Inst. Chem. Eng.* **2018**, 92, 8–14.
- (16) Chien Dang, M.; Dung Dang, T. M.; Fribourg-Blanc, E. Silver Nanoparticles Ink Synthesis for Conductive Patterns Fabrication Using Inkjet Printing Technology. *Adv. Nat. Sci. Nanosci. Nanotechnol.* **2015**, 6 (1).
- (17) Tang, X. F.; Yang, Z. G.; Wang, W. J. A Simple Way of Preparing High-Concentration and High-Purity Nano Copper Colloid for Conductive Ink in Inkjet Printing Technology. *Colloids Surfaces A Physicochem. Eng. Asp.* **2010**, 360 (1–3), 99–104.
- (18) Kamyshny, A. Metal-Based Inkjet Inks for Printed Electronics. *Open Appl. Phys. J.* **2011**, 4 (1), 19–36.
- (19) Walker, S. Synthesis and Patterning of Reactive Silver Inks. **2013**.
- (20) Raut, N. C.; Al-Shamery, K. Inkjet Printing Metals on Flexible Materials for Plastic and Paper Electronics. *Journal of Materials Chemistry C*. 2018.
- (21) Chen, J. J.; Zhang, J.; Wang, Y.; Guo, Y. L.; Feng, Z. S. A Particle-Free Silver Precursor Ink Useful for Inkjet Printing to Fabricate Highly Conductive Patterns. *J. Mater. Chem. C* **2016**, 4 (44).
- (22) Black, K.; Singh, J.; Mehta, D.; Sung, S.; Sutcliffe, C. J.; Chalker, P. R. Silver Ink Formulations for Sinter-Free Printing of Conductive Films. *Sci. Rep.* **2016**, 6 (October 2015), 1–7.
- (23) Yang, W.; Wang, C.; Arrighi, V. An Organic Silver Complex Conductive Ink Using Both Decomposition and Self-Reduction Mechanisms in Film Formation. *J. Mater. Sci. Mater. Electron.* **2018**, 29 (4).
- (24) PASQUARELLI, R.; Curtis, C.; Van Hest, M. Inkjet Printing of Nickel and Silver Metal Solar Cell Contacts. *Energy J.* **2007**, 91–96.
- (25) Li, D.; Sutton, D.; Burgess, A.; Graham, D.; Calvert, P. D. Conductive Copper and Nickel Lines via Reactive Inkjet Printing. *J. Mater. Chem.* **2009**, 19 (22), 3719–3724.
- (26) Petukhov, D. I.; Kirikova, M. N.; Bessonov, A. A.; Bailey, M. J. A. Nickel and Copper Conductive Patterns Fabricated by Reactive Inkjet Printing Combined with Electroless Plating. *Mater. Lett.* **2014**, 132, 302–306.

- (27) Ginley, D. S.; Curtis, C. J.; Miedaner, A.; Maria van Hest, M. F. A.; Kaydanova, T. (12) United States Patent (10) Patent No .: US 8641931 B2, 2014.
- (28) Mallory, G. O.; Hajdu, J. B. The Fundamental Aspects of Electroless Nickel Plating. In *Electroless Plating: Fundamentals and Applications*; Noyes Publications: Norwich, NY, 1990; pp 1–56.
- (29) Sudagar, J.; Lian, J.; Sha, W. Electroless Nickel, Alloy, Composite and Nano Coatings - A Critical Review. *J. Alloys Compd.* **2013**, *571*, 183–204.
- (30) Wu, Z. G.; Munoz, M.; Montero, O. The Synthesis of Nickel Nanoparticles by Hydrazine Reduction. *Adv. Powder Technol.* **2010**, *21* (2), 165–168.
- (31) Nik Roselina, N. R.; Azizan, A. Ni Nanoparticles: Study of Particles Formation and Agglomeration. *Procedia Eng.* **2012**, *41*, 1620–1626.
- (32) Nik Roselina, N. R.; Azizan, A.; Hyie, K. M.; Jumahat, A.; Abu Bakar, M. A. Effect of PH on Formation of Nickel Nanostructures through Chemical Reduction Method. *Procedia Eng.* **2013**, *68*, 43–48.
- (33) Kim, K. H.; Lee, Y. B.; Choi, E. Y.; Park, H. C.; Park, S. S. Synthesis of Nickel Powders from Various Aqueous Media through Chemical Reduction Method. *Mater. Chem. Phys.* **2004**, *86* (2–3), 420–424.
- (34) Tientong, J.; Garcia, S.; Thurber, C. R.; Golden, T. D. Synthesis of Nickel and Nickel Hydroxide Nanopowders by Simplified Chemical Reduction. *J. Nanotechnol.* **2014**, *2014*.
- (35) Li, Z.; Han, C.; Shen, J. Reduction of Ni²⁺ by Hydrazine in Solution for the Preparation of Nickel Nano-Particles. *J. Mater. Sci.* **2006**, *41* (11), 3473–3480.
- (36) Chandra, S.; Kumar, A.; Tomar, P. K. Synthesis of Ni Nanoparticles and Their Characterizations. *J. Saudi Chem. Soc.* **2014**, *18* (5), 437–442.
- (37) Sun, Y.; Mayers, B.; Herricks, T.; Xia, Y. Polyol Synthesis of Uniform Silver Nanowires: A Plausible Growth Mechanism and the Supporting Evidence. *Nano Lett.* **2003**, *3* (7), 955–960.
- (38) Dong, H.; Chen, Y. C.; Feldmann, C. Polyol Synthesis of Nanoparticles: Status and Options Regarding Metals, Oxides, Chalcogenides, and Non-Metal Elements. *Green Chem.* **2015**, *17* (8), 4107–4132.
- (39) Fievet, F.; Lagier, J. P.; Figlarz, M. Preparing Monodisperse Metal Powders in Micrometer and Submicrometer Sizes by the Polyol Process. *MRS Bull.* **1989**, *14* (12), 29–34.

- (40) Gustafsson, M.; Fischer, A.; Ilyukhin, A.; Maliarik, M.; Nordblad, P. Novel Polynuclear Nickel(II) Complex: Hydrazine, Sulfato, and Hydroxo Bridging in an Unusual Metal Hexamer. Crystal Structure and Magnetic Properties of $[\text{Ni}_6(\text{N}_2\text{H}_4)_6(\text{SO}_4)_4(\text{OH})_2(\text{H}_2\text{O})_8](\text{SO}_4)(\text{H}_2\text{O})_{10}$. *Inorg. Chem.* **2010**.